

ADENO-ASSOCIATED VIRUS VECTORED  
IMMUNOPROPHYLAXIS AGAINST *PLASMODIUM FALCIPARUM*

by

Renuka Elizabeth Joseph

A thesis submitted to Johns Hopkins University in conformity with the requirements for  
the degree of Master of Science

Baltimore, Maryland

October, 2016

© 2016 Renuka Elizabeth Joseph  
All Rights Reserved

## Abstract

Anti-Circumsporozoite protein (CSP) monoclonal antibodies (mAbs) can neutralize *Plasmodium* sporozoites *in vitro* and passively transferred mAb against *P. falciparum* CSP can block liver invasion by sporozoites of a transgenic rodent parasite that expresses chimeric *P. falciparum* CSP (*Pb-Pf*), preventing infection in mice. Despite this, attempts at targeting CSP for a vaccine have fallen short of expectations, mainly since a single un-neutralized sporozoite can cause disease, necessitating sustained high-titer neutralizing antibodies which current vaccines have been unable to achieve.

Recently, David Baltimore's laboratory developed adeno-associated virus type 8 (AAV8) platform that efficiently delivers pre-formed mAb genes *in vivo* and directs sustained, high-level mAb production. We have adopted this technology to express humanized mAbs against the N-terminal region of the CSP protein of *P. falciparum* in mice. Mice developed high titer human IgG antibodies as early as one week post-transduction, and levels have remained constant for more than six weeks at 800 to 1000 µg of IgG/mL. Mice transduced with humanized CSP mAb 5D5 (5D5-AAV) and challenged intravenously with 10<sup>4</sup> transgenic *P. berghei* parasite expressing complete *P. falciparum* CSP (*Pb-PfCSP*) sporozoites, exhibited a statistically significant decrease in liver parasite burden. Unexpectedly, no protection or delay to parasitemia was observed in mice challenged by infective *Pb-PfCSP* mosquito bites.

Neutralizing antibodies against the vector used in mAb delivery (Vectored Immunoprophylaxis; VIP) can inhibit expression of mAb. Neutralizing antibodies in the sera of *Aotus* monkeys previously transduced with AAV1, -7 and -8 vectors were detected using an AAV-luciferase assay. Based on the results of the assay, a correlation between high pre-existing neutralizing anti-AAV antibodies titers and inhibition of AAV vectored mAb expression was noted. Our results recommend the prescreening of animals for neutralizing anti-AAV antibodies before VIP administration.

## Acknowledgments

It has always been my dream to work with malaria and what better place to start than Johns Hopkins. The reality of the dream however I learnt was quite different. Leaving my country, family, friends and adapting to the new system education was a daunting task, but I reached the end of my master's degree. This was made possible by the support and encouragement of many people.

I would like to thank my advisor, Dr. Gary Ketner, who was a true mentor to me and I cannot thank him enough for his constant guidance and support. His door was always open whether it be to discuss one of my new ideas or my future. His trust in my abilities made me have faith in myself and taught me how to be an independent researcher. I consider it a great privilege to have worked and learnt under him. I would also like to thank Brendan Dolan and Harrison Powell for making the lab such a lively environment and for always helping me when I needed it. A special mention to Dr. Cailin Deal whose previous work with the VIP project made my job easier.

I would like to thank Dr. Photini Sinnis, who was also the first person to introduce me to malaria research. Her vast knowledge and mentorship helped me expand my skill set, and I am also grateful to her for being my secondary reader. I would also like to thank the other members of the Sinnis lab – Dr. Daniel Ragheb, Dr. Christine Hopp, Maya Aleshnick and especially Amanda Balaban, who continued helping me even after I left the Sinnis Lab.

I would like to express my sincere gratitude to Dr. Christian Munoz, Olivia Hunt and especially Dr. Victoria Baxter for teaching me and helping me with my mice experiments. A special mention to the members of the Griffin lab who advised me on my experiments and kept me company when I was alone in the Ketner lab. Thank you to the parasite and insectary core for the mosquitoes and also to Liedos Inc. for the 5D5 monoclonal antibody data.

To my friends – Sarah, Megan, Jennifer, Katie, Arthur, Nicole, Sujana and Sam thank you for getting me out of the lab and making my graduate studies here an enjoyable experience. To Simba the dog, Finlay and Simba the cat, thank you for being the best stressbusters in the world. Finally, I would like to thank my family especially my parents for always being there for me. Amma and Appa, thank you for working so hard so that my dreams could come true.

# TABLE OF CONTENTS

Abstract.....	ii
Acknowledgments.....	iii
List of Figures .....	vi
Introduction.....	1
Plasmodium lifecycle.....	1
Pre-erythrocytic vaccine rationale and vaccines.....	3
Adeno-associated Virus .....	7
Adeno – associated virus vectors in gene therapy .....	10
Pre-existing immunity.....	12
Materials and Methods.....	15
Construction and Cloning of VIP plasmids .....	15
Validation of the Functionality of the 5D5 VIP plasmid .....	17
Production and purification of AAV VIP virus .....	17
AAV quantification.....	19
AAV intramuscular injection and serum collection.....	19
Quantification of antibody production by ELISA.....	20
Parasite.....	21
Pb/Pf CSP Challenge .....	21
Luciferase assay to detect neutralizing antibodies against AAV .....	22
Data analysis .....	23
Results.....	27
Construction and Cloning of VIP plasmids .....	27
In vitro validation of the Functionality of the 5D5 VIP plasmid .....	29
In vivo characterization of 5D5 VIP vectors .....	29
Pb-PfCSP Challenge .....	30
Luciferase assay to detect neutralizing antibodies against AAV .....	31
Discussion.....	48
References.....	55
Curriculum Vitae .....	75

## List of Figures

Figure 1: Stages of the malarial life cycle that are vaccine targets. ....	14
Figure 2: Schematic representation of VIP expression vector. ....	24
Figure 3: Schematic representation of 5D5 monoclonal antibody binding site on CSP. ....	26
Figure 4: Confirmation of 5D5H-2A10, 5D5L-2A10 and 5D5 VIP plasmid clones by restriction digestion. ....	34
Figure 5: Schematic representation of b12 transgene, 2A10 transgene, 5D5H-2A10 transgene, 5D5L-2A10 transgene and 5D5 transgene in VIP expression vector. ....	36
Figure 6: Cloned VIP plasmids expressing high quantity of human IgG antibodies in vitro. ....	38
Figure 7: 5D5-AAV8 expresses high levels of sustained human IgG antibody in vivo, and VIP-produced Plasmodium falciparum antibodies retain ability to recognize CSP. ....	39
Figure 8: VIP administration significantly reduces parasite burden in the liver. ....	40
Figure 9: VIP did not provide sterile protection to mice challenged by infected mosquito bite ...	41
Figure 10: Neutralizing antibody titers against AAV1 affect the expression of VIP in Aotus monkeys. ....	42
Figure 11: VIP mAb expressed for a short period in Aotus monkeys having low neutralizing activity against AAV8. ....	43
Figure 12: High neutralization activity against AAV7 inhibits the expression of VIP mAb in Aotus monkeys. ....	45
Figure 13: Pre-screening of ten Aotus monkey sera for anti-AAV neutralizing antibodies against AAV1, -8 and -7. ....	47

## Introduction

Malaria is an infectious disease that is caused by a single-celled protozoan of the genus *Plasmodium*. Despite tremendous efforts, malaria remains a significant global health problem with about 3.2 billion people still at risk from this parasitic disease<sup>1</sup>. The WHO estimates that there were 214 million cases of malaria in 2015 and 438 000 deaths<sup>1</sup>. The majority of these cases and deaths occur in Sub-Saharan Africa where there is a stable transmission of this disease all year round<sup>2</sup>. However, Latin America, Asia and to some extent the Middle East and Europe, are at risk as well<sup>1</sup>.

The high prevalence of malaria and the disease burden it causes has made it a prime target for eradication programs. The current arsenal of tools against malaria include insecticides, bed nets, drainage of marshes and other sources of stagnant water and anti-malarial drugs like chloroquine and artemisinin. Chloroquine was an effective antimalarial drug until the 1950s, but now most malarial strains are resistant to this drug<sup>3</sup>. Artemisinin, another antimalarial drug was found to be extremely effective in treating people with malaria and was found to be effective against strains that were resistant to chloroquine. However, partial resistance to this antimalarial drug is now emerging<sup>4,5</sup>. With the spread of anti-malarial drug-resistant *Plasmodium* strains that need for an effective vaccine against malaria is imminent.

### *Plasmodium* lifecycle

Malaria belongs to the phylum apicomplexa, which also includes *Babesia*, *Cryptosporidium*, and *Toxoplasma*. The members of this phylum have complex lifecycle involving both asexual and sexual reproductive stages. The vector for *Plasmodium* is the female *Anopheles* mosquito, and it is here the sexual reproduction of the parasite occurs<sup>6</sup>. When a female *Anopheles* mosquito takes a blood meal from a human infected with malaria, the mosquito ingests gametocytes along with the blood meal<sup>6</sup>. Gametocytes are the sexual reproductive stage of the parasite, which are present

in the circulation of an infected human host<sup>6</sup>. External cues and drop in temperature in the mosquitoes promote the gametocytes to mature into haploid male and female gametes<sup>7</sup>. In the midgut, these haploid male and female gametes fuse to form diploid zygotes that develop into ookinetes<sup>6</sup>. The ookinete is motile and can transverse through the midgut wall of the mosquito till it reaches the basal lamina where it develops into the next lifecycle stage called the oocyst<sup>6</sup>. Oocyst are where the haploid sporozoites are produced and multiply to large numbers<sup>6</sup>. The sporozoites are elongated and reach a length of about 10  $\mu\text{m}$  and have a diameter of about 1  $\mu\text{m}$ , and this is the infective stage of the parasite life cycle<sup>8</sup>. When the sporozoites reach maturity, they are released from the oocyst into the hemocoel and circulate in the hemolymph of the mosquito. Some of these circulating sporozoites come in contact with the salivary glands, and approximately 15% of the circulating sporozoites will invade the salivary gland<sup>9</sup>. During the mosquito's next blood meal, the salivary gland sporozoites are injected into the skin of the human host as it probes for blood<sup>10</sup>. A small portion of these sporozoites then find and invade a blood vessel<sup>11</sup> and are carried to the liver by the blood flow. When reaching the liver, the sporozoites exit the blood circulation transverse across the sinusoid cell layer to infect hepatocytes<sup>12</sup>. Here, the sporozoites develop and mature into the exoerythrocytic schizont form in which thousands of hepatic merozoites are formed<sup>12</sup>. Rupture of these mature schizonts releases 2,000 to 40,000 merozoites, and each of these merozoites can infect an erythrocyte cell in the host<sup>12</sup>. The merozoites in the erythrocytes develop into trophozoites and replicate in an asexual process called schizogony to form 10-14 merozoites<sup>10</sup>. The erythrocytes containing the merozoites rupture and the released merozoites invade new erythrocytes. The release of these merozoites from erythrocytes coincides with the cyclic fever which is characteristic of malaria<sup>13</sup>. A portion of the merozoites develop into the sexual stage of the parasite – gametocytes which are taken up by the vector as it takes a blood meal from the infected human host<sup>6</sup>.

There are many members in the *Plasmodium* genus, but only five are known to infect humans.



These include *Plasmodium falciparum*, *P. vivax*, *P. ovale*, *P. malariae* and *P. knowlesi*. *P. knowlesi* was recently added to the list as a primate malaria but can cause infections in humans<sup>14</sup>. *P. vivax* and *P. ovale*, can cause relapse due to persistent liver forms of the parasite that can remain dormant for months to years<sup>6</sup>. *P. falciparum* is the predominant *Plasmodium* species in Sub-Saharan African where the majority of deaths due to malaria occurs<sup>1</sup>. *P. falciparum* infect erythrocytes of all ages<sup>15</sup> which leads to a higher parasite density in the blood of the host compared to those infected with the other *Plasmodium* species. The high levels of parasitemia during *P. falciparum* infection can lead to severe anemia due to the rupture of the infected erythrocytes<sup>6</sup>. *P. falciparum* infected erythrocytes are also thought to have the ability to adhere to the surrounding vasculature to prevent splenic disruption. The adherence of the parasite-infected cells can lead to the blockage of blood vessels and the blockage of the brain vasculature is known as cerebral malaria<sup>6</sup>. Cerebral malaria and severe anemia are clinical manifestations of severe malaria which is common among *P. falciparum* infected individuals, especially children under the age of five years<sup>6</sup>. Most current vaccine development efforts are targeted against *P. falciparum* which causes the most deaths compared to the other human *Plasmodium* species.

#### *Pre-erythrocytic vaccine rationale and vaccines*

Current malaria vaccine development efforts have been focused on three different stages of the *Plasmodium* life cycle: the pre-erythrocytic stage that consists of the sporozoites in the skin and the liver stage, the erythrocytic phase that involves the invasion and asexual reproduction of the parasite within red blood cells (RBCs), and finally, the transmission stage that involves gametocyte uptake and further development of the parasite within the mosquito (figure 1)<sup>16</sup>. In comparison to the other stages, vaccines directed against the pre-erythrocytic phase of the parasite can prevent both the manifestation of disease and the transmission of the parasite by inducing an immune response against the sporozoites and/or the liver stage that will neutralize sporozoites and prevent invasion of hepatocytes and/or the induction of CD8+ T cells that can recognize and

kill infected hepatocytes<sup>17-19</sup>. The number of sporozoites transmitted by a mosquito into the host is around 10 - 120 sporozoites, based on a 3 minute feeding time<sup>20,21</sup> and a vaccine that can neutralize all these injected sporozoites can lead to sterile immunity.

Vaccines that are under current development mainly target the circumsporozoite protein (CSP), thrombospondin-related adhesion protein (TRAP) which is essential for sporozoite motility and invasion<sup>22,23</sup> and liver-stage antigen (LSA) which plays a role in the differentiation of the parasite in the liver<sup>24,25</sup>. The main goal of a vaccine is to provide sterile immunity against the disease and in the case of malaria, this has been achieved by inoculation with radiation-attenuated sporozoites<sup>19,26,27</sup>. To achieve sterile immunity by the use of irradiated sporozoites requires individuals to be bitten by roughly 1000 irradiated infectious mosquitoes or receive five intravenous injections (i.v) of irradiated sporozoites<sup>19,28</sup>. These methods of inoculation are tedious, require skilled labor and the sporozoites need to be maintained in cold-chain storage to ensure their vitality. These limitations and other logistical issues have made this vaccine impractical for global use.

Studies conducted on immune responses induced by irradiated sporozoites have helped elucidate the mechanism by which the immune response provides protection. The majority of the research has shown that the predominant immune response in irradiated sporozoite vaccinated volunteers was antibodies directed against CSP<sup>29</sup>. CSP covers the surface of sporozoites and is implicated in sporozoite development, adhesion, and migration<sup>30-33</sup>. CSP consists of three main regions – a central repeat domain bound by a C-Terminal region containing a type I thrombospondin repeat (TSR) motif on one side and an N-terminal portion containing a conserved proteolytic cleavage site on the opposite side<sup>6</sup>. Studies have shown that the majority of anti-CSP antibodies recognized the central (NANP)<sub>3</sub> region in *P.falciparum* CSP<sup>34</sup>, a B cell epitope that varies among *Plasmodium* species but is highly conserved in isolates of the same species from different geographical regions<sup>35</sup>. Passive transfer of monoclonal antibodies that recognize this B cell

epitope have shown to be protective against the disease in both mouse and non-human primate (NHP) models<sup>36</sup>. However, sporozoites do not spend a lot of time in the skin (1 to 2 hrs., though some leave within minutes)<sup>37</sup> and blood before invading the liver, limiting the interaction between the neutralizing antibodies and the sporozoites. To overcome this issue, a sustained high level of anti-CSP specific antibodies is required for a solely humoral-based protective immune response.

In July 2015, a pre-erythrocytic malaria vaccine called RTS, S/AS01 was approved by the European Medicines Agency (EMA) becoming the first vaccine against malaria or any parasitic disease to be licensed. EMA has recommended the vaccine to be used in young children (6 weeks to 17 months) in areas where *P. falciparum* is prevalent<sup>38</sup>. RTS, S malaria vaccine was developed by GlaxoSmithKline (GSK) in collaboration with Walter Reed Army Institute for Research and PATH Malaria Vaccine Initiative (MVI). The vaccine consists of a hepatitis B surface antigen (HBsAg) fused to 19 copies of the central repeat region and C-terminal flanking region of *P. falciparum* mixed with unfused HBsAg<sup>39</sup>. This recombinant CSP consists of both B and T cell epitopes capable of inducing both neutralizing antibodies and cell-mediated immunity against the sporozoite and the liver stage<sup>39</sup>. Preliminary evaluation of the RTS, S vaccine showed that the addition of a novel oil-in-water adjuvant, ASO1, which was later optimized to the Monophosphoryl lipid A (MPL) and QS-21 bearing adjuvant ASO2 increased the antibody response to the vaccine<sup>40,41</sup>. A phase III clinical trial for RTS, S was conducted in 11 different sites in Africa where children (5–17 months) and infants (6–12 weeks) were given three doses of the vaccine in a randomized manner<sup>42</sup>. Vaccine efficacy against clinical malaria in children 20 months after dose one was found to be 45%. The vaccine efficacy was found to be 46% in children, 18 months after dose 3 was administered<sup>42</sup>. The vaccine efficacy against malaria hospitalization, severe malaria and all-cause hospitalization in children was found to be 41%, 34%, and 19% respectively<sup>42</sup>. In infants (6–12 weeks), the vaccine efficacy was found to be lower (27%) and did not show significant protection against malaria hospitalization, severe malaria, and

all-cause hospitalization<sup>42</sup>. Vaccine efficacy was found to wane over time as well<sup>42</sup>. The addition of a booster dose increased the efficacy of the vaccine in both children and infants<sup>43</sup>. RTS, S has a low vaccine efficacy but is still capable of averting some clinical malaria and severe malaria cases and can help reduce the burden of disease in Africa. It has also paved the way for the development of second-generation malaria vaccines.

An alternate method of vaccination is the use of viral vectors to deliver genes into a host. An adeno-associated virus vectored Immunoprophylaxis (VIP) vaccine expressing neutralizing antibody 2A10 or 2C11 was developed and tested in the Ketner lab. 2A10, and 2C11 are anti-*P. falciparum* CSP monoclonal antibodies that recognize the central NANP repeat region in *P. falciparum* CSP<sup>44,45</sup> and are protective if passively transferred to naive mice. 2A10-AVV or 2C11-AVV ( $1 \times 10^{11}$  genome copies) were injected intramuscularly (i.m) into the cranial thigh muscle in mice and these mice expressed human Immunoglobulin G (hIgG) levels between 100 to 500  $\mu\text{g/mL}$  in serum (some mice had hIgG levels up to 1200  $\mu\text{g/mL}$  in their serum) which was sustained until the end of the study (52 weeks)<sup>45</sup>. 2A10-AAV and 2C11-AVV transduced mice showed a significant decrease in liver parasite burden when challenged with transgenic *P. berghei* sporozoites containing a chimeric CSP gene bearing the *P. falciparum* CSP central repeat (*Pb/Pf*), injected intravenously ( $1.0 \times 10^4$ -  $2 \times 10^4$  sporozoites per mouse)<sup>45</sup>. 2A10-AAV and 2C11-AVV transduced mice were also challenged by infected mosquito bites and 60% of 2A10-AAV and 30% of 2C11-AAV transduced mice showed sterile protection and the other mice in these groups showed delayed parasitemia compared to the control group<sup>45</sup>. All mice transduced by 2A10-AAV expressing hIgG levels  $> 1000 \mu\text{g/mL}$  in their serum showed sterile protection against disease<sup>45</sup>. This alternative method has showed promise and further studies in NHP models and the use of other monoclonal antibodies in the VIP system are ongoing.

### *Adeno-associated Virus*

AAV is a small (~25nm) Single stranded DNA virus in the parvovirus family that belongs to the genus Dependovirus. AAV is a nonenveloped virus, and its capsid is composed of three proteins-VP1, VP2 and VP3 arranged in T=1 icosahedral symmetry. Each Capsid consists of 60 protein subunits and these proteins VP1-3, are present in 1:1:10 proportion<sup>46</sup>. The Core of each VP has a conserved structure that consists of an eight stranded  $\beta$ -barrel motifs ( $\beta$ B to  $\beta$ I) and an  $\alpha$ -helix ( $\alpha$ A). AAV have long loop insertions that connect the core  $\beta$ -barrel strands and these loops cluster at the surface forming nine conformational variable regions (VRI-VRIX) that lead to local variations in the capsid surface<sup>46,47</sup>. These different conformations of the variable regions are thought to influences the tissue transduction efficiency, cellular tropism and antigenic reactivity between the various AAV serotypes<sup>47-50</sup>.

The AAV single stranded DNA genome is around 4.7 kb and is flanked by an inverted terminal repeat (ITR) sequences of about 145 nucleotides on either side<sup>51</sup>. The ITRs arrange into a T-shaped, base-paired hairpin structure which contain important *cis*-elements for viral encapsulation and replication<sup>52</sup>. They also contains *cis*-elements required for viral genome integration and rescue from host chromosomal DNA<sup>53</sup>. The genome consists of two genes, the rep (transcription regulated by promoters p5 and p19) that encodes four non-structural proteins (Rep-78, -52, -68 and -40) formed by alternative mRNA splicing, crucial for viral replication, and the cap gene (transcription regulated by promotor p40) that encodes the three structural proteins (VP1-3) that constitute the AAV capsid. Rep78 and Rep68 play a role in the regulation of viral and cellular promoters, viral replication, site-specific integration and rescue of integrated AAV genome<sup>54-60</sup>. Rep52 and Rep40, are important for accumulation of viral DNA for packaging into new AAV particles<sup>61</sup>. All four Rep proteins have helicase and ATPase activity<sup>62,63</sup>.

The different AAVs are known to bind to a variety of cell receptors on their target cell in the host. AAV2,-3 and -6 bind heparan sulfate proteoglycan receptors on the cell, while AAV1, -4, -5 and -

6 bind sialic acid and AAV9 binds galactose<sup>64</sup>. AAV2 is also known to use fibroblast growth factor receptor 1<sup>65</sup>. AAV serotype 8 which was isolated in rhesus macaques uses the 37/67 KD Laminin receptor (LamR) to help bind to its target cells<sup>66</sup>. LamR binds AAV3, -9 and -2 as well<sup>66</sup>. After binding to their receptor, AAV2 is taken into the target cell by clathrin-mediated endocytosis which is aided by  $\alpha_v\beta_5$  integrin<sup>67</sup>. The virus is eventually released into the cytosol and penetrates into the nucleus through the nuclear pore complex (NPC)<sup>68</sup>. Inside the nucleus, the virus can go into a latent state or through a lytic cycle depending on the presence or absence helper viruses - adenovirus or herpes simplex virus. In the presence of helper virus function, AAV replication is productive and consists of three main steps: the conversion of the single stranded viral DNA genome into a double stranded template for transcription, unidirectional strand-displacement replication and terminal resolution of self-annealed ITRs<sup>69</sup>. Transcription of the rep genes occur first as it plays a significant role in both positive (in the presence of helper effects) and negative regulation of transcription<sup>54</sup>. Helper virus co-infection activates promoters p5 and p19 which leads to the transcription of Rep68, -78, -52 and -40 and after Rep proteins are transcribed, extensive DNA replication occurs<sup>55,56,70,71</sup>. AAV goes through unidirectional strand displacement replication for the replication of its DNA and the ITRs on either sides of the DNA have motifs – the Rep binding site (RBS) and Terminal resolution site (TRS) that serve as the viral origin of replication<sup>72,73</sup>. The ITRs have the ability to self-anneal and provide a base-paired 3' hydroxyl group for unidirectional DNA synthesis. The host replication machinery including polymerase  $\delta$  along with some components from the helper virus mediates DNA synthesis<sup>74–76</sup>. After DNA synthesis, terminal resolution occurs to replicate the self-annealed ITR. This process is mediated by the Rep proteins that bind to the RBS motif within the ITR and leads to a site- and strand-specific nick at the TRS that regenerates a 3' hydroxyl end<sup>77</sup>. The newly synthesized 3' hydroxyl end enables replication through the viral ITR<sup>77</sup>. At the end of the replication cycle, there are two possible products - a single-stranded full-length AAV displacement product and a double-

stranded full-length AAV genome. The roles of these products are still unknown, but it is thought that the single-stranded AAV genome might serve as a template for further replication and the double-stranded replication product may act as a template for genome packaging<sup>69</sup>.

In the absence of helper virus factors, there is a limited expression of Rep68/78 which leads to the repression of AAV genome, inhibition of DNA replication and integration of viral DNA into the host genome<sup>54</sup>. The integrated AAV genome can be rescued by coinfection of a latently infected cell with a helper virus<sup>78</sup>. Integration of viral DNA into host genome can result in upregulation of genes and tumorigenesis which is a safety concern. Many *in vitro* studies have been conducted to investigate the mechanism and biological effects of AAV DNA integration into the host genome. Wild type (WT) AAV was found to integrate most frequently in a site-specific manner on the chromosome 19q13.42, also known as AAVS1<sup>79,80</sup>. This site-specific integration is rep dependent<sup>81</sup> which is not present in rAAV used for gene therapy and other therapeutics. Other integration hotspots include sites on chromosome 5p13.3 (AAVS2) and chromosome 3p24.3 (AAVS3)<sup>82</sup>. In contrast, *In vivo* studies have shown the WT AAV DNA integrates at a low frequency and majority of the DNA exists as double stranded episomes in human tissue<sup>83</sup>. rAAV lacks many components of WT AAV, like the Rep proteins but are still found to integrate into the host genome at low frequency which can potentially lead to genotoxicity<sup>84</sup>. The results of a study conducted in mice showed the presence of integrated AAV vector proviruses in four different tumors from four different mice. All these integrated AAVs were mapped to a 6-kb region of chromosome 12 (AAV-HCC locus), and no AAV DNA was found in the surrounding normal tissue suggesting that integration of AAV vector may lead to cancer in certain situation including the age of the mice and type of AAV vector used<sup>85</sup>. A recent study to test the safety and site-specific integration of rAAV vectors was done using the EMA licensed AAV1-LPL<sup>S447X</sup> vector which was developed for the treatment of lipoprotein lipase deficiency (LPLD). Tissue from human and mice subjects that had previously received one or more doses of AAV1-LPL<sup>S447X</sup>

administered i.m was used to map the vector integration sites in the host genome. In the human samples, two vector integration hotspots- one within the *PCBD2* gene and the other near the gene *OR4F29* in the nuclear genome were identified<sup>86</sup>. However, the majority of the vector integration sites were in the mitochondrial DNA (mtDNA) compared to the nuclear genome<sup>86</sup>. The hotspots for vector integration in mice were found to be near the *Col19a1* gene (composed of mtDNA-homologous sequences), the muscle-specific gene *Ttn* and in the *Myh* gene in the nuclear genome<sup>86</sup>. Specific mtDNA enrichment combined with direct sequencing performed on one mouse sample showed that majority of the vector integration sites (12 out of 20) occurred within a nuclear mitochondrial DNA region (Similar sequences present in both mitochondrial and nuclear genomes )<sup>86</sup>. No significant vector genome integration was noted in the *AAVSI* locus (common integration site of WT AAV) or the AAV-HCC locus (implicated in AAV integration-mediated formation of hepatocellular carcinoma)<sup>86</sup>. These results indicate that use of rAAV vector is safe and could be used to treat of mitochondrial disorders by gene therapy. There are still some concerns about using AAV vectors in humans and it is an active field of study, and that is continuing to grow as rAAV use increases.

#### *Adeno – associated virus vectors in gene therapy*

Adeno-associated virus (AAV) was first discovered in 1965<sup>87</sup> and with the understanding of the basic biology of AAV and its ability to infect a wide variety of tissues have promoted the development of recombinant adeno-associated virus vectors (rAAV) that are now being used in gene therapy frequently. The extensive use of rAAV in gene therapy is due to its low immunogenicity, lack of pathogenicity of the wild-type (WT) virus, ability to transduce a broad range of dividing and non-dividing cell types and its ability to maintain long-term gene expression after transduction. Around twelve human AAV serotypes and more than a hundred NPH AAV serotypes have been identified<sup>88</sup>. AAV serotype 2 (AAV2) was the first AAV serotypes to discovered and characterized. For this reason, rAAV2 was used as a vector to treat



hemophilia B, cystic fibrosis, Parkinson's disease, rheumatoid arthritis, age-related macular degeneration, Batten disease, Leber's congenital amaurosis and Canavan's disease<sup>89</sup>. Clinical efficacy of AAV based gene therapy was first noted when patients suffering from Leber's congenital amaurosis, an autosomal recessive disease that causes congenital blindness, were treated with rAAV2-RPE65 and showed improved vision and sensitivity to light for four to six years<sup>90-93</sup>. Parkinson's and congenital aromatic L-amino acid decarboxylase (AADC) deficiency were treated with the rAAV2-AADC vector; the results indicated improved gross motor development in both trials<sup>94,95</sup>.

An important realization in AAV-mediated gene therapy was that the different AAV serotypes have different transduction efficiencies for certain tissues. Transduction with AAV8 vectors in skeletal muscles and cardiac muscles, results in systemic gene transfer in these tissues as AAV8 can efficiently cross the blood barrier compared to the other AAV serotypes in mice and hamsters<sup>96</sup>. AAV1 was found to have a higher transduction efficiency for skeletal muscles than AAV2<sup>97</sup>. AAV6 and AAV5 transduce murine airway epithelial more efficiently than the other AAV serotypes<sup>98</sup>. The understanding of the various tissue tropisms of the different AAV serotypes and the formation of hybrid vectors with AAV2 replication genes and capsids of other serotypes have led to the development of more efficient vectors<sup>99</sup>. Pseudotyped (foreign DNA encapsulated by viral capsid proteins) AAV8 vector expressing factor IX has some success in treating hemophilia B<sup>100</sup>. rAAV1-lipoprotein lipase (LPL) administered i.m was found to decrease pancreatitis and serum cholesterol levels in patients suffering from lipoprotein lipase deficiency<sup>101</sup>. In 2012, rAAV1-LPL was licensed in Europe<sup>102</sup> and it opened up opportunities for the continued study of AAV as a tool for gene therapy and vaccine development.

### *Pre-existing immunity*

rAAV vector mediated gene transfer has shown promise as a therapeutic for many diseases. An obstacle to this treatment approach is the presence of pre-existing neutralizing anti-AAV antibodies and acquired antibodies generated after treatment with rAAVs that can reduce or inhibit the efficiency of these therapeutics, especially if the vector needs to be administered repeatedly<sup>103,104</sup>. Around 30-80% of the world's population is estimated to be seropositive for anti-AAV antibodies against AAV1 and -2, with anti-AAV2 being the most prevalent<sup>105</sup>. A study conducted in France with serum samples of small human cohort concluded that the prevalence of neutralizing antibodies against AAV5, -6 and -9 was around 50 % and AAV8 had a seroprevalence of less than 40%<sup>106</sup>. Non-neutralizing antibodies that are capable of binding AAV can also inhibit vector transduction by activating the immune system and clearing the vector from the host<sup>107</sup>. The development of this humoral response to AAV is thought to occur early in life around the age of two as a consequence of WT AAV exposure<sup>108,109</sup>. Additionally, newborn babies have been found to have maternal anti-AAV antibodies that decrease few months after birth but increase again<sup>108,109</sup>. These studies show that the time frame where individuals are naive to anti-AAV is narrow, making it difficult to administer AAV vectored therapeutics.

Humoral response mounted against WT AAV leads to the production of all four IgG subclasses with IgG1 being predominant<sup>106,110,111</sup>. Lower IgG2 levels were also present in the anti-AAV specific antibody response and the highest levels of IgG2 were found against AAV8<sup>106</sup>. IgG3 and IgG4 levels were low and variable with AAV6 inducing the highest IgG3 response<sup>106</sup>. Another problem imposed by anti-AAV antibodies is their ability to cross-react with a broad range of AAV serotypes<sup>106</sup>. This is mostly due the high degree of amino acid conservation among AAVs<sup>112</sup>. Characterization of the immune response against AAV can help in understanding and overcoming the problem presented by this immune response against rAAV vectored gene transfer therapeutics.

Most Studies use Enzyme-linked Immunosorbent assay (ELISA) to determine the anti-AAV antibody titers in serum. The disadvantage of using this test to detect antibody titers is that it cannot distinguish between neutralizing and non-neutralizing antibodies. Cell based assays have been developed to the better estimate the neutralizing activity of anti-AAV antibodies in a host. The development of more sensitive tests can be used to detect naive individuals for AAV vectored therapeutics or help decide which AAV serotype should be used as a vector. Other methods to overcome the presence of neutralizing anti-AAV antibodies include the development of novel, artificial AAV vectors<sup>113</sup>, plasmapheresis<sup>114</sup>, transient immunosuppression<sup>115,116</sup>, delivery of the vector with isolated perfusion and saline flushing<sup>117</sup> and modulation of antibody responses with empty capsids<sup>118</sup>.

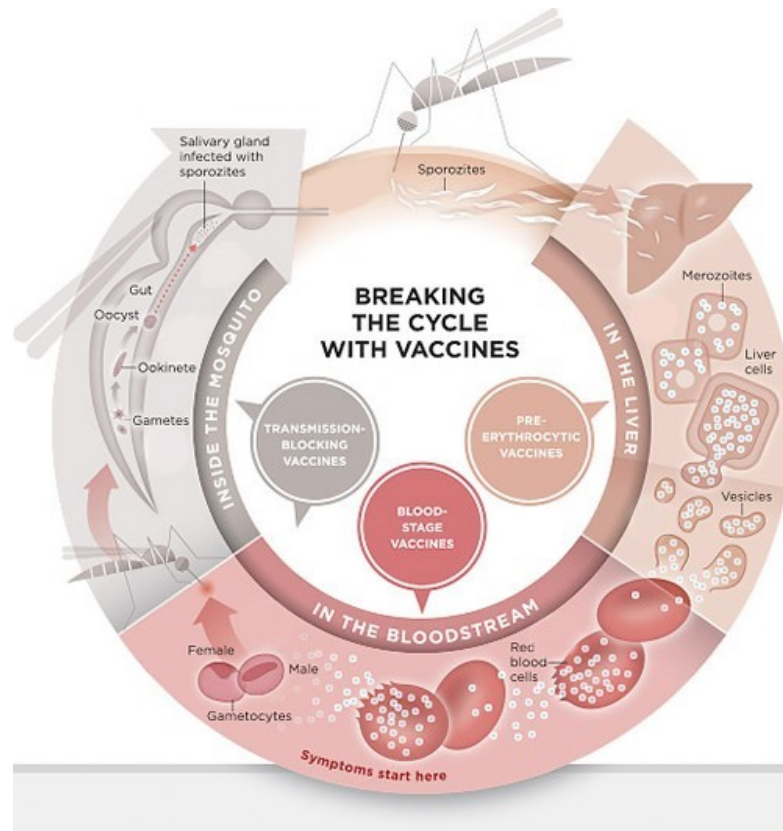


**Figure 1: Stages of the malarial life cycle that are vaccine targets.**

Pre-erythrocytic vaccines targeting antigens expressed on sporozoites or infected hepatocytes can prevent both disease and transmission. Blood-stage vaccines targeting antigens expressed on merozoites and infected red blood cells work to reduce disease severity and transmission blocking vaccines targeting either gametocytes or developmental stages within the mosquito prevent transmission of the *Plasmodium* parasite.

## Materials and Methods

### *Construction and Cloning of VIP plasmids*

To express b12 (anti-HIV-1 gp120) and 2A10 (anti-*P. falciparum* CSP) antibodies in mice, the DNA sequences of the variable regions of these antibodies were synthesized from published sequences<sup>119</sup> and cloned into the VIP expression vector as previously described (Figure 2)<sup>120,121</sup>. This was done in Dr. David Baltimore's laboratory at California Institute of Technology by Dr. Alex Balazs and tested further by Dr. Cailin Deal in Dr. Gary Ketner's laboratory at Johns Hopkins Bloomberg school of Public Health. These previously studied VIP expression vector plasmids were used in this study as controls.

5D5, an anti-*P.falciparum* CSP monoclonal antibody that specifically binds to a linear epitope EDNEKLRKPKH near the proteolytic cleavage site in the N-terminus region of *P.falciparum* 3D7 CSP (Figure 3)<sup>122</sup> was produced by Leidos Inc and the DNA sequences of the variable regions of 5D5 mAb were provided by Aragen Biosciences Inc. To test the effects of 5D5 mAb against transgenic *P. berghei* expressing complete *P. falciparum* CSP using VIP system, the variable region DNA sequences of 5D5 mAb were cloned into the previously characterized 2A10 VIP expression vector, replacing the 2A10 mAb variable DNA sequences. The 5D5 mAb variable light (V<sub>L</sub>) and heavy (V<sub>H</sub>) chain DNA sequences were compared to that of 2A10 in the VIP expression vector, to determine the insertion site for the 5D5 mAb sequence in the VIP expression vector using a software called DNA Strider. 5D5 V<sub>L</sub> and V<sub>H</sub> chain insert sequences were synthesized by GeneArt. The synthesized 5D5 V<sub>H</sub> chain insert sequence was flanked by built-in restriction sites for *NotI* and *AgeI*, and the synthesized 5D5 V<sub>L</sub> chain insert sequence was flanked by built-in restriction sites for *NsiI* and *PvuII*. Restriction digestion was carried out with 20 µg of plasmid DNA containing the 5D5 V<sub>H</sub> insert sequence and 20 µg of plasmid DNA

containing the 5D5 V<sub>L</sub> chain insert sequence. These reactions were incubated at 37°C for 2 hours (h) and run on a 1% agarose gel containing 0.5 µg/mL ethidium bromide at 50mA with a 100bp ladder (Invitrogen). The QIAquick Gel Extraction Kit (Qiagen) was used to extract and purify the 5D5 V<sub>H</sub> and V<sub>L</sub> insert DNA from the agarose gel. The amount of extracted insert DNA was determined by nanodrop spectrometer. In two separate reactions, 20 µg of backbone 2A10 VIP plasmid was digested using *NotI* and *AgeI* (to remove 2A10 V<sub>H</sub> sequence from the VIP plasmid) and *NsiI* and *PvuII* (to remove 2A10 V<sub>L</sub> sequence from the VIP plasmid). These reactions were incubated at 37°C for 2h. 5µl sample of each reaction was run on a 1% agarose gel containing 0.5 µg/mL ethidium bromide at 50mA with a 100bp ladder. The restriction enzymes in the two reactions were heat-inactivated by heating the reactions at 65°C for 20 minutes (mins). The digested vector DNA was dephosphorylated by adding Shrimp Alkaline Phosphatase (New England Biolabs) and incubating at 37°C for 1h. The Shrimp Alkaline Phosphatase was heat inactivated by heating the reactions at 65°C for 5 mins. The digested 2A10 VIP vector DNA without 2A10 V<sub>H</sub> chain and the 5D5 V<sub>H</sub> insert DNA ligated using T4 ligase (New England Biolabs) to form the 5D5H-2A10 plasmid. The Vector to insert DNA ratio in the ligation reaction was 1:4 and was incubated overnight at 16°C<sup>123</sup>. The T4 ligase was heat inactivated by heating the reaction at 65°C for 10 mins. The same ligation process was followed for the digested 2A10 VIP vector DNA without 2A10 V<sub>L</sub> chain and 5D5 V<sub>L</sub> insert DNA to form the 5D5L-2A10 plasmid. The new plasmids were transformed into DH5α competent cells (MAX Efficiency DH5α competent cells ThermoFisher Scientific) and plated on Luria Broth (LB) plates containing 60µg/mL of ampicillin and incubated at 37°C for 24h<sup>123</sup>. Selected colonies were grown in LB broth containing 60µg/mL of ampicillin for 24hrs at 37°C, and plasmid DNA was extracted from these cultures using Qiagen Plasmid plus kit. Restriction Digestion and sequencing were done to confirm the correct insertion of 5D5 V<sub>H</sub> and 5D5 V<sub>L</sub> sequences in the 5D5H-2A10 and the 5D5L-

2A10 plasmids respectively. 5D5H-2A10 plasmid was used as the backbone to construct the 5D5 VIP plasmid containing both 5D5 V<sub>H</sub> and V<sub>L</sub> chain sequences. The 5D5H-2A10 plasmid digested with restriction enzymes NsiI and PuvII to remove the 2A10 V<sub>L</sub> chain sequence and the 5D5 V<sub>L</sub> insert DNA was inserted into this plasmid using the same method as previously mentioned. Restriction Digestion and sequencing were done to confirm the correct insertion of 5D5 V<sub>H</sub> and V<sub>L</sub> chain in the newly formed 5D5 VIP plasmid. All plasmid stocks and DNA were stored in the -80.

#### *Validation of the Functionality of the 5D5 VIP plasmid*

To validate the functional activity of the 5D5 VIP plasmid, 293T cells (human embryonic kidney cells) were grown in modified Minimum Essential Media (MEM) containing 10% Fetal Bovine serum (FBS), 1% Penicillin-Streptomycin mixture (P/S) and 1% L-glutamine (L-Glu) in a 12 well tissue culture plate (Corning), until the cells reached 70-80% confluency. 293T cells were transfected with 1µg of 2A10 VIP plasmid, 5D5 VIP plasmid, 5D5H-2A10 plasmid and 5D5L-2A10 plasmid DNA in duplicates using transfection reagent BioT (Bioland Scientific). Two wells were not transfected with DNA and were used as a negative control. 48h post-transfection, 50 µL of supernatant was pipetted out of each well and quantified for total human IgG production by ELISA<sup>120</sup>.

#### *Production and purification of AAV VIP virus*

The method followed to prepare AAV vector virus expressing 5D5 mAb or luciferase has been previously described<sup>120</sup>. Three days before transfection, four 15 cm plates were seeded with  $3.75 \times 10^6$  293T cells each in 25 mL of modified MEM and these plates were maintained in a 5% CO<sub>2</sub> incubator at 37 °C. 2 or more hours before transfection, the media in the plates were removed and 15mL of Dulbecco's

Modified essential media (DMEM) containing 10%FBS,1%P/S and 1% L-Glu (media will be referred to as D10) was added. 197µg of pAAV DNA, 98.4µg of helper vectors pHELP DNA (Applied Viromics) and 24.6µg of 5D5 VIP plasmid DNA (or luciferase for luciferase assay) were mixed together in a 50mL tube. To 16mL of DMEM (no serum), 240µl BioT was added and vortexed. The DNA was mixed with the BioT DMEM mixture, vortexed and incubated for 5mins at room temperature. 4mL of this reaction was added to each 15cm plate containing 293T cells. The supernatant was collected at five time points -36, 48, 72, 96 and 120 h, passed through a 0.22µm filter (Millipore) and stored in 4°C. 15mL of fresh D10 media was added to the plates every time the supernatant was collected. The collected supernatant was split into two glass bottles (~150mL each) and 37.5 mL of 5×PEG solution (40% polyethylene glycol, 2.5 M NaCl) was added to each bottle and the virus was allowed to precipitate on ice for 24h in 4°C. The solution was centrifuged (Sorvall RC5C centrifuge) at 5000 RPM for 30mins at 4°C and the supernatant was removed. The pellets were re-suspended using 1.37 g/mL caesium chloride solution and the solution was transferred to two Sorvall quick seal tubes. The solution was centrifuged (Sorvall WX ultracentrifuge) at 60,000 RPM for 24h at 20°C. Fractions of the centrifuged solution were collected (100-150µl per well) in a 96 well flat bottom plate and the refractive index of these fraction were determined using a refractometer. Fraction with a refractive index between 1.3755 and 1.3655 were combined and the final volume was made up to 15mL by adding Test Formulation Buffer 2 (TFB2, 100 mM sodium citrate, 10 mM Tris pH 8). The solution was pipetted on to a 100 kDa MWCO



centrifugal filter (Millipore) and centrifuged at 3000 RPM (Sorvall legend RT series centrifuge) at 4°C for 30-45 mins or till the retentate was below the 1mL mark. The virus was washed three times by adding 15mL of TFB2 each time to the filter and repeated centrifugation. The membranes were washed with 300µl of TFB2 and the final retentate was aliquoted and stored at -80 °C.

#### *AAV quantification*

The quantification AAV vectors has been previously described <sup>120</sup>. The unknown AAV virus and standard sample (AAV8 virus expressing b12 mAb-1x10<sup>12</sup>GC/mL) were diluted tenfold in DNase buffer and 10 units of DNase I (Roche) was added to each sample. The samples were incubated at 37°C for 30 mins. The Unknown AAV samples were diluted in DPEC treated water to 1:1000, 1:10000 and 1:100000. The Standard curve was created by diluting the standard sample four-fold in DPEC treated water from 2x10<sup>10</sup> GC/mL to 0 GC/mL. A PCR mix containing 8.2µL of SYBR green, 2µL of DPEC treated water and 0.33µL of forward and reverse primers (5' CMV: AACGCCAATAGGGACTTTCC and 3' CMV: GGGCGTACTTGGCATATGAT or the luciferase transgene (5' Luc: ACGTGCAAAAGAAGCTACCG and 3' Luc: AATGGGAAGTCACGAAGGTG) per sample was prepared. 10µl of PCR mix and 5µL of sample were added to the 96 well PCR plate. The samples were run in duplicates in the MicroAmp Fast Optical 96-Well Reaction Plate. The amount Virus in the samples were quantified using a quantitative PCR (Applied Biosystems One Step Plus qPCR) with the program: one cycle of 50 °C for 2 mins, one cycle of 95 °C for 10 min, 40 cycles of 95 °C for 15 seconds (s) and 60 °C for 60s.

#### *AAV intramuscular injection and serum collection*

Aliquots of previously titered viruses were thawed on ice and diluted in TFB2 to achieve the predetermined dose of  $1 \times 10^{11}$  genome copies in a 50  $\mu$ L volume. Inbred 3-to 4 week old C57BL/6 (Jackson Laboratories) female mice, in groups of four or ten, were given a single 50  $\mu$ L intramuscular (i.m.) injection into the cranial thigh muscle with a 29G needle. At various times after vector administration, blood was collected from the cheek vein into serum separator tubes (BD). Tubes were spun for 10 minutes at 5,000 RPM to separate sera from red blood cells. Sera was collected and stored at  $-80^{\circ}\text{C}$ .

#### *Quantification of antibody production by ELISA*

For the detection of total human IgG, ELISA plates were coated with 0.1  $\mu$ g per 100  $\mu$ L per well of goat anti- human IgG-Fc antibody (Bethyl) overnight <sup>120</sup>. Plates were washed three times with TBS containing 0.1% Tween20 (TBS-T) and three times with TBS followed by blocking with 200  $\mu$ L 1% BSA (Sigma) in TBS (TBS-1% BSA) per well for 1h. Samples were serially diluted three-fold in TBS-1% BSA starting at 1:1500. 100  $\mu$ L of each sample dilution was added to the plate and incubated for 1h at room temperature (RT). Plates were washed as above and incubated with 100  $\mu$ L per well TBS-1% BSA diluted HRP- conjugated goat anti-human kappa light chain antibody (1:10,000; Bethyl) for 1h at RT. Plates were washed a final time and 100  $\mu$ L of ABTS Peroxidase Substrate System (KPL) was added per well. The plate was incubated in the dark for 15 minutes at RT. The reaction was stopped by adding 100  $\mu$ L 2M sulphuric acid per well. Using Human Reference Serum (Bethyl), a standard curve was generated and mouse pre-bleed sera were used to establish background. Plates were read at a wavelength of 450nm using a Molecular Devices Emax microplate reader.

For the detection of anti-CSP antibodies, plates were coated with 0.05  $\mu$ g per well of *P.*

*falciparum* CSP purified from MR-272 plasmid (Malaria Reference and Research Resource MR-272) overnight <sup>124</sup>. All subsequent steps are described above except a standard curve was not

utilized. The positive control used was Purified 2A10 and the dilution at which the optical density value was two times greater than the blank was reported as the endpoint titer.

### *Parasite*

Transgenic murine *Plasmodium berghei* sporozoites expressing the complete human *P. falciparum* CSP (*Pb-PfCSP*) were used in all the experiments. The transgenic parasite was developed by Dr. Diego A. Espinosa in Zavala laboratory. The parasite was ordered through the parasite core at Johns Hopkins Bloomberg School of Public Health.

### *Pb/Pf CSP Challenge*

C57BL/6 mice were used for the experiments since they have been shown to be highly susceptible to sporozoite challenge<sup>125</sup>. Infected *Anopheles stephensi* mosquitoes were anesthetized on ice and transferred to a petri dish containing 70% ethanol for 30s. The mosquitoes were then transferred to a plate filled with Hank's balanced salt solution (HBSS, invitrogen) containing 1% mouse serum. The salivary glands were dissected out under a light microscope using a 25G needle. The dissected salivary glands were transferred to an Eppendorf tube along with the dissection media and kept on ice. The salivary glands were crushed and the amount of sporozoites present in the supernatant was counted using a hemocytometer. Mice were challenged intravenously with  $1.0 \times 10^4$  transgenic *Pb-PfCSP* parasites<sup>126</sup>. Approximately 38.5h later, mice were euthanized to assess parasite burden in livers. Whole livers were homogenized in denaturing solution (4m Guanidine Thiocyanate, 25mM Sodium Citrate pH 7, 0.5%N lauryl sarcosine and  $\beta$ -mercaptoethanol), and RNA was extracted as previously described<sup>127,128</sup>. The total RNA in the samples were determined by nanodrop spectrometer and diluted to a final concentration of 100ng/mL for cDNA synthesis. After cDNA synthesis, parasite loads were determined by qPCR for *P. berghei* 18S rRNA<sup>129</sup> and mouse GAPDH was used as an internal control.

For the assessment of sterile protection, *Anopheles stephensi* mosquitoes infected with *Pb-PfCSP* parasites were starved overnight. Mice were anesthetized with 300 to 350  $\mu$ L of 2% avertin and were subjected to feeding from 5-8 mosquitoes for 10 minutes. The number of mosquitoes that fed on each mouse was noted, based on the presence of blood in the midgut after dissection. Starting from day 4, blood smears were made daily until day 14 by nicking the tail of each mouse and collecting blood, and these smears were observed under a microscope for blood stage parasites. Smears were fixed with methanol before staining with a 10% Giemsa stain solution (Sigma-Aldrich) for 20 mins. The slides were observed under 100x magnification under a light microscope. The day post infection that blood stage parasitemia was evident was recorded as the day of patency. After confirmation of parasitemia, mice were euthanized. Mice were considered to be sterilely protected if there was no evidence of parasitemia by day 14.

#### *Luciferase assay to detect neutralizing antibodies against AAV*

The detection of neutralizing antibodies against AAV was done as previously described<sup>130</sup> with some modifications. 2V6.11 cells<sup>131</sup> were diluted to  $2 \times 10^5$  cells/mL in DMEM media containing 10% heat inactivated FBS, 1% P/S and without phenol red. Ponasterone A was added to the cell containing media at a final concentration of  $1 \mu\text{g/mL}$ . 100 $\mu$ L of this solution was added per well into a black 96 well flat bottom tissue culture plate (UltraCruz) and incubated overnight in a 37°C, 5% CO<sub>2</sub> incubator. Serum samples were diluted 1:3.16 times in heat inactivated FBS. Previously titrated viruses expressing luciferase were diluted in TFB2 to a concentration of  $5 \times 10^9$  GC/mL. 20 $\mu$ L of the diluted serum samples were mixed with 20 $\mu$ L of the diluted virus and incubated for 1h in a 37°C, 5% CO<sub>2</sub> incubator. As a negative control or minimum neutralization control, 20 $\mu$ L of the diluted virus was added to 20 $\mu$ L of FBS and incubated along with the other samples. 7.5 $\mu$ L of each sample and control was added per well to the tissue culture containing the 2V6.11 cells and incubated overnight in a 37°C, 5% CO<sub>2</sub> incubator. Samples were added in duplicates or

triplicates. 100  $\mu$ L of Bright-Glo luciferase assay system (Promega) was added per well in the tissue culture plate and allowed to sit at RT for 3 mins. Luminescence of each sample was read using IVIS spectrum in vivo imaging system. The first dilution to show 90% or above neutralization activity was reported as the titer of neutralization antibodies in the sample against AAV.

#### *Data analysis*

DNA sequence comparison, homology and restriction site identification were performed using a DNA analysis software called DNA Strider. The majority of data and statistical analysis were performed using Prism software (GraphPad 5) using a Mann–Whitney U test. Differences were found to be significant when p was less than 0.05. Kaplan-Meier day to patency curves were analyzed using a logrank test.

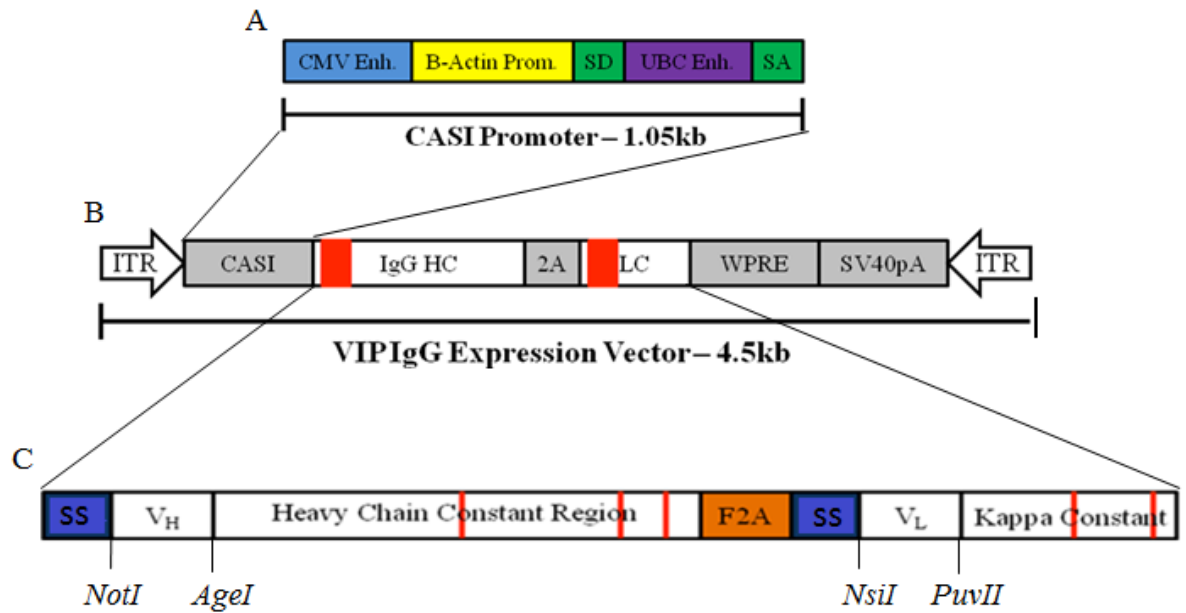


**Figure 2: Schematic representation of VIP expression vector.**

(A) The novel CASI promoter combines the cytomegalovirus (CMV) enhancer and chicken  $\beta$ -actin promoter followed by a splice donor (SD) and splice acceptor (SA) flanking the ubiquitin (UBC) enhancer region. (B) The VIP expression vector for antibody expression indicating the AAV2 inverted terminal repeats (ITR), the CASI promoter, an IgG1 heavy chain linked to the light chain separated by a self-processing 2A sequence, a woodchuck hepatitis posttranscriptional regulatory element (WPRE) and an SV40 polyadenylation signal (SV40pA). Antibody variable regions of the heavy and light chains are colored in red (C) Schematic representation of the IgG1 transgene that was optimized for expression in vitro. Highlighted in blue is the human growth hormone (HGH) derived signal sequence (SS) and the F2A self-processing peptide (orange), yielding in separate heavy and light chains. Red lines mark the predicted splice donor and acceptor sites that

have been mutated. The Variable heavy chain ( $V_H$ ) is flanked by *NotI* and *AgeI* restriction sites and the Variable light chain ( $V_L$ ) is flanked by *NsiI* and *PvuII* restriction sites.

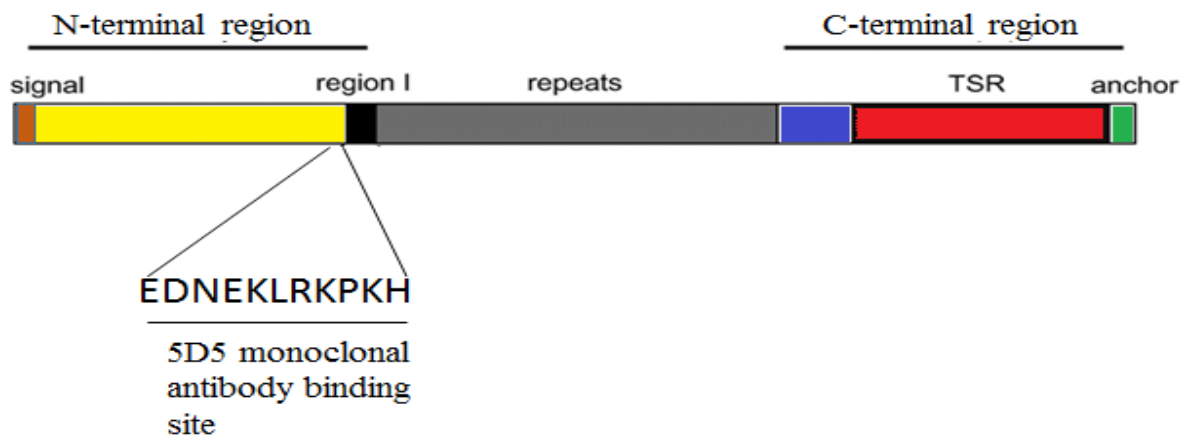


**Figure 3: Schematic representation of 5D5 monoclonal antibody binding site on CSP.**

CSP consists of three main regions – a central repeat domain (grey box) bound by a C-Terminal region containing a type I thrombospondin repeat (TSR) motif (red box) and GPI anchor site (green box) on one side and an N-terminal portion containing a conserved proteolytic cleavage site called region I (black box) and a signal sequence (brown box) on the opposite side<sup>6</sup>. 5D5, an anti-*P.falciparum* CSP monoclonal antibody binds to a linear epitope EDNEKLRKPKH near the proteolytic cleavage site (region I) in the N-terminus region of *P.falciparum* 3D7 CSP<sup>122</sup>.



## Results

### *Construction and Cloning of VIP plasmids*

After decades of research, the only malaria vaccine to be licensed is the RTS, S/ASO1 in areas of active *P.falciparum* transmission<sup>38</sup>. The vaccine has an efficacy below 50% in the target population and the effectiveness of the vaccine wanes over time<sup>42,43</sup>. It is known that CSP antibodies alone can neutralize and prevent infection by sporozoites, but this requires very high sustained levels of antibody in the host<sup>36,44</sup>. Recently, it has been demonstrated that genes encoding anti – *P.falciparum* CSP antibodies 2A10 and 2C11 delivered to mice by a newly-designed AAV8 vector can direct long-lived high-level mAb production. The same vaccination strategy has been shown to be successful against HIV in mice. This approach termed vectored immunoprophylaxis (VIP) is potentially applicable to any disease against which an antibody response alone is protective<sup>120,121</sup>.

The positive results of the 2A10 and 2C11 VIP vector systems have encouraged the study of other monoclonal antibodies that may inhibit *P. falciparum* infection using the VIP vaccine strategy. 5D5 is an anti-*P.falciparum* CSP monoclonal antibody that specifically binds to a linear epitope EDNEKLRKPKH near the proteolytic cleavage site in the N-terminus region of *P.falciparum* 3D7 CSP, inhibiting the CSP processing<sup>122</sup>. Proteolytic cleavage of the CSP is necessary for parasite infection of the liver.

Using 2A10 VIP vector plasmid as a backbone the 5D5 V<sub>H</sub> and V<sub>L</sub> chain sequences were inserted into the VIP vector plasmid replacing 2A10 sequences. Comparison of the V<sub>H</sub> chain sequence of 2A10 in the VIP plasmid and 5D5 V<sub>H</sub> chain sequence revealed the presence of a signal peptide and cleavage site at one end and sequence homology at constant region the other end. The same was noted when V<sub>L</sub> chain sequences of 2A10 in the VIP plasmid and 5D5 were compared. Signal peptides are important for the transport of newly synthesized proteins in the cell and mutations in

the signal peptide sequence can decrease the secretion efficiency of the antibody<sup>132</sup>. To avoid mutation of the signal peptide, The 5D5 V<sub>H</sub> and V<sub>L</sub> chains were inserted between the signal peptide cleavage site and sites of sequence homology between 2A10 and 5D5. The area where sequence homology between 2A10 and 5D5 was observed indicates the location of the constant region of the IgG1 chains which are highly conserved between different IgG1 antibodies<sup>133</sup>. Based on this information, synthetic DNA sequences encoding the 5D5 heavy and light variable regions, flanked by built-in restriction sites for *NotI* and *AgeI* (heavy) and *NsiI* and *PvuII* (light) were prepared. Clones containing the synthetic 5D5 V<sub>H</sub> and V<sub>L</sub> insert synthetic DNAs were digested and the V<sub>H</sub> and V<sub>L</sub> inserts were purified by electrophoresis and gel extraction. Restriction digestion of the backbone 2A10 VIP plasmid with *NotI* and *AgeI* resulted in 2 bands, ~5873bp and ~540bp. The 5873bp band was the 2A10 VIP plasmid without the 2A10 V<sub>H</sub> chain, and the 540bp band was the 2A10 V<sub>H</sub> chain digested out of the plasmid as predicted by DNA analysis software DNA Strider. Restriction digestion of the backbone 2A10 VIP plasmid with *NsiI* and *PvuII* resulted in 2 bands, ~5819bp and ~598bp. The 5819bp band was the 2A10 VIP plasmid without the 2A10 V<sub>L</sub> chain, and the 598bp band was the 2A10 V<sub>L</sub> chain digested out of the plasmid as predicted by DNA analysis software DNA Strider. No other bands were observed on the gel indicating the complete digestion of the backbone 2A10 VIP plasmid (not shown). The insert DNAs 5D5 V<sub>H</sub> and V<sub>L</sub> insert DNAs were ligated to 2A10 VIP plasmid without 2A10 V<sub>H</sub> chain and 2A10 VIP plasmid without 2A10 V<sub>L</sub> chain respectively to form 5D5H-2A10 Plasmid and 5D5L-2A10 plasmid. The correct insertion of these insert DNAs in their respective digested 2A10 plasmids was determined by restriction digestion and sequencing. Restriction digestion of the 5D5H-2A10 plasmid with *NsiI* and *BglIII* restriction enzymes resulted in 2 bands, ~5281bp and ~1132bp each (figure 4A). The sizes of these bands were unique to 5D5H-2A10 plasmid digested by *NsiI* and *BglIII*. Restriction digestion of the 5D5L-2A10 plasmid with restriction enzymes *DraIII* and *XcmI* resulted in 2 bands, ~4758bp and ~1659bp. The sizes of these bands were unique to 5D5L-2A10 plasmid digested by *DraIII* and *XcmI* (figure 4B). The size of all the

bands observed on the gel were identical to the sizes predicted by DNA Strider sequence analysis software, indicating the correct insertion of the insert DNAs in the 2A10 VIP plasmids.

Sequencing of the 5D5H-2A10 plasmid and 5D5L-2A10 further confirmed the correct insertion of the insert DNAs in the digested 2A10 plasmid.

The 5D5 VIP plasmid was prepared using 5D5H-2A10 plasmid as the backbone. The correct insertion of 5D5 V<sub>L</sub> insert DNA into 5D5H-2A10 plasmid was determined by restriction digestion and sequencing. Restriction digestion of the 5D5 VIP Plasmid with restriction enzymes *DraIII* and *XcmI* resulted in 2 bands, ~4758bp and ~1659bp each (figure 4C). The size of the bands observed on the gel were identical to the sizes predicted by DNA analysis software DNA Strider, indicating the correct insertion of the insert DNAs in the 2A10 VIP plasmids. Sequencing of the 5D5 VIP further confirmed the correct insertion of the insert DNAs in the digested 2A10 plasmid. The schematic diagram of b12 VIP vector transgene, 2A10 VIP Vector transgene, 5D5L-2A10 VIP vector transgene, 5D5H-2A10 VIP vector transgene and 5D5 VIP vector transgene present in their respective VIP expression vectors are shown in Figure 5.

#### *In vitro validation of the Functionality of the 5D5 VIP plasmid*

The 5D5 VIP plasmid, 5D5H-2A10, 5D5L-2A10 and 2A10 VIP plasmids were characterized *in vitro* for human IgG antibody expression in the supernatant of transfected 293T cells (Figure 6). All four plasmids produced human IgG at ~0.86 µg/mL indicating no loss of function of the VIP plasmid after cloning. With this confirmation AAV vectors with the capsid from serotype 8 were made that expressed the humanized IgG mAb 5D5.

#### *In vivo characterization of 5D5 VIP vectors*

To determine expression by these VIP vectors *in vivo*, 11 C57BL/6 mice were injected intramuscularly in the cranial thigh muscle with  $1 \times 10^{11}$  genome copies (GC) of 5D5-AAV, b12-AAV (AAV expressing HIV mAb b12, Baltimore lab) or media alone. Within one week post

transduction, all AAV-transduced mice expressed between 100-200 µg/mL of human IgG antibodies. Expression continued to increase till 3 weeks post transduction and was sustained out to 6 weeks (Figure 7A). The antibody concentration was maintained between 800-1000 µg/mL in all mice. To ensure that the initial manipulation of the CSP-specific mAb did not affect their ability to bind to CSP, sera from transduced mice were used to probe recombinant CSP by ELISA (Figure 7B). 5D5 transduced mice expressed antibodies that bound to recombinant CSP with similar kinetics as human IgG antibody expression (Figure 7B). Sera from b12-AAV mice and media alone mice did not recognize recombinant CSP, demonstrating the specificity of the 5D5 antibody.

### *Pb-PfCSP Challenge*

To test the ability of VIP to protect mice from challenge *in vivo*,  $1.0 \times 10^4$  *Pb-PfCSP* sporozoites isolated from infected *Anopheles stephensi* mosquitoes were injected i.v. into the tail vein of 20 mice six weeks post transduction with 5D5-AAV or b12-AAV vectors. Antibodies specific for CSP block liver invasion by sporozoites. Therefore, mice were sacrificed 38.5h post infection, a time when viable sporozoites will have successfully invaded and replicated in liver cells. RNA was extracted from liver homogenates, followed by cDNA synthesis and finally qPCR was used to quantify the *P. berghei* 18S rRNA copies in the liver to reflect the parasite burden. In two independent experiments, 5D5 mice had a statistically significant reduction in parasite burden as compared to b12-AAV mice (data for one experiment is shown in Figure 8).

In the mosquito bite challenge experiment, the infectivity of the mosquito cage was estimated to be 80 % by dissecting a limited number of salivary glands (n=10) and checking for the presence of sporozoites. 4-5 mosquitoes fed on each 5D5-AAV and b12-AAV transduced mouse. This was determined by dissecting the midgut to check for blood. 4 days post challenge, blood stage parasitemia was observed in all b12-AAV and 5D5 transduced mice (Figure 9B). All the mice challenged in this experiment had 700-1000 µg/mL of human IgG in their sera (Figure 9A). The

experiment was repeated and the same results were noted again.

### *Luciferase assay to detect neutralizing antibodies against AAV*

Pre-existing neutralizing anti-AAV antibodies and acquired antibodies generated after treatment with rAAVs can reduce or inhibit the efficiency of AAV vectored therapeutics, especially if the vector need to administered repeatedly<sup>103,104</sup>.

Four *Aotus* monkeys referred to as A304, A336, A312 and A247 were transduced with an AAV vector expressing 2A10. A304 and A336 were transduced with 2A10-AAV1. A312 and A247 were transduced with 2A10-AAV8 and 6 months later they were transduced again with 2A10-AAV7. The monkey serums were tested for vector-encoded anti-CSP antibody expression by ELISA done by Dr. Gary Ketner. A304 transduced with AAV1 expressing 2A10, produced anti-CSP antibodies up to 15 weeks post transduction (Figure 10A). The other 2A10-AAV1-transduced monkey, A336, showed low levels of anti-CSP until week three after which the anti-CSP antibody expression declined until it was no longer detectable (Figure 10A). Anti-CSP antibodies present in the sera of *Aotus* monkeys 312 and 247 transduced with AAV8 expressing 2A10 mAb expressed anti –CSP antibodies at varying amounts until no anti-CSP antibodies were detected 7 weeks post transduction (Figure 11A). A312 had peak levels of anti-CSP antibodies at week 2 after which the antibody levels declined (Figure 11A). Anti-CSP antibodies levels peaked at week 5 for A247 after which it declined (Figure 11A). *Aotus* monkeys 312 and 247 transduced with 2A10-AAV7, 6 months post transduction with AAV8 did not express detectable levels of anti– CSP antibodies (Figure 12A). One hypothesis for the failure to express 2A10 mAb in some of the *Aotus* is that the presence of pre-existing anti-AAV neutralizing antibodies against the AAV vectors, inhibited the efficient transduction of the vector.

To investigate that possibility, an assay was developed to detect anti-AAV neutralizing antibodies against different AAV serotypes using vectors expressing luciferase. The sera of A304 and A336

before and after immunization with 2A10-AAV1 was tested and A304 pre-bleed had lower neutralizing activity compared to A336. A336 showed 90% neutralizing activity up to dilution 1:1000 (Figure 10B) and A304 showed 90% neutralizing activity up to dilution 1:316 (Figure 10B). After immunization with 2A10-AAV1 the neutralizing activity of A304 increased and the neutralization percentage did not fall below 90% even at the 1:3160 dilution (highest dilution) (Figure 10B). A336 showed a slight increase in neutralizing activity as well, post 2A10-AAV1 transduction (Figure 10B).

The sera of A312 and A247 before and after immunization with 2A10-AAV8 were tested for anti-AAV8 neutralizing antibodies (Figure 11B). Pre-bleeds of both A312 and A247 monkeys that were administered had neutralizing activity below 40% at 1:10 dilution which increased after immunization with 2A10-AAV8 to above 95% (Figure 11B). The neutralizing activity against AAV8 increased further in both monkeys after immunization with 2A10-AAV7 (6 months post 2A10-AAV8 transduction) which can be observed in the higher dilutions (1:100 to 1:3160) (Figure 11B). The sera of A312 and A247 before and after immunization with 2A10-AAV7 were tested for anti-AAV7 neutralizing antibodies (Figure 12B). Pre-bleeds of both monkeys had high neutralizing activity (above 90%) (Figure 12B). Immunization with 2A10-AAV8 (6 months before 2A10-AAV7 transduction) did not change the neutralizing percentage against AAV7 in either monkey (Figure 12B). However, neutralizing activity against AAV7 increased in both monkeys post 2A10-AAV7 immunization (Figure 12B). These results seem to confirm the hypothesis that anti-AAV antibodies inhibit 2A10-AAV expression and the need to pre-screening animals for pre-existing anti-AAV antibodies before VIP administration. Pre-bleeds sera from ten *Aotus* monkeys were obtained prior to selection of the four *Aotus* described above. These sera were diluted to 1:316 and were screened for neutralizing antibodies against AAV1, -8 and -7 (Figure 13). The cutoff neutralization value above which no VIP expression would occur was estimated to be 90% based on the 2A10-AAV1 neutralizing antibody experiments mentioned

previously. Out of the ten monkeys, only A336 had a neutralizing activity above 90% against AAV1. All ten monkeys had neutralizing activity below 90% against AAV8 (Figure 13), suggesting that the 90% cutoff may be too high for AAV8. Four of the ten monkeys had neutralizing activity above 90% against AAV7 (A304, A312, A418 and A247).

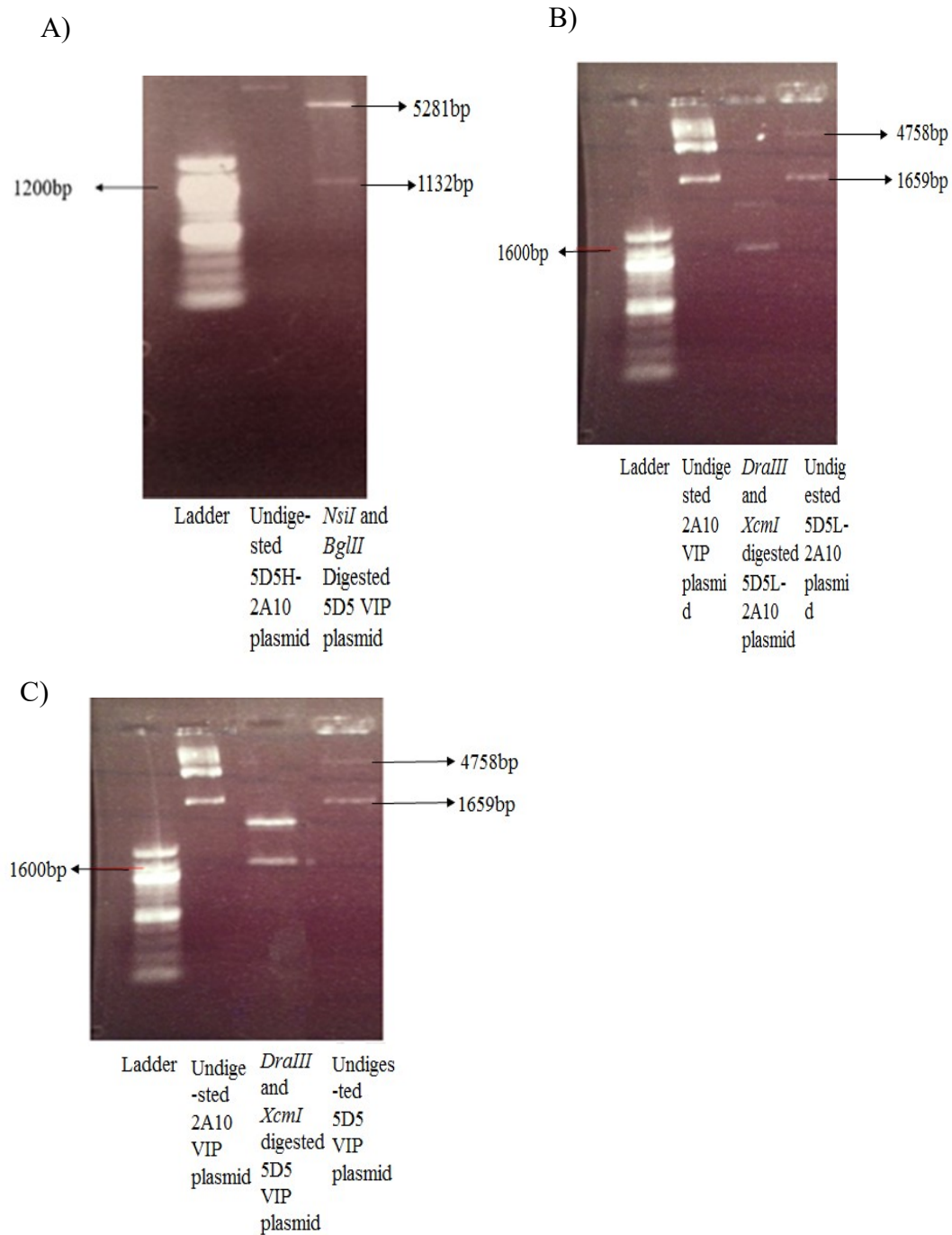


**Figure 4: Confirmation of 5D5H-2A10, 5D5L-2A10 and 5D5 VIP plasmid clones by restriction digestion.**

Restriction digestion of (A) 5D5H-2A10, (B) 5D5L-2A10 and (C) 5D5 VIP plasmid at unique restriction sites to confirm the correct insertion of 5D5 V<sub>H</sub> and V<sub>L</sub> chains in the 2A10 VIP plasmid. Restriction digestion of 5D5H-2A10 plasmid with *NsiI* and *BglII* resulted in a 2 bands,



5281bp and 1132bp each. Restriction digestion of 5D5L-2A10 plasmid with *DraIII* and *XcmI* resulted in 2 bands, 4758bp and 1659bp. Restriction digestion of the 5D5 VIP Plasmid with *DraIII* and *XcmI* resulted in a 2 bands, 4758bp and 1659bp. These bands match the sizes predicted by DNA analysis software DNA Strider.

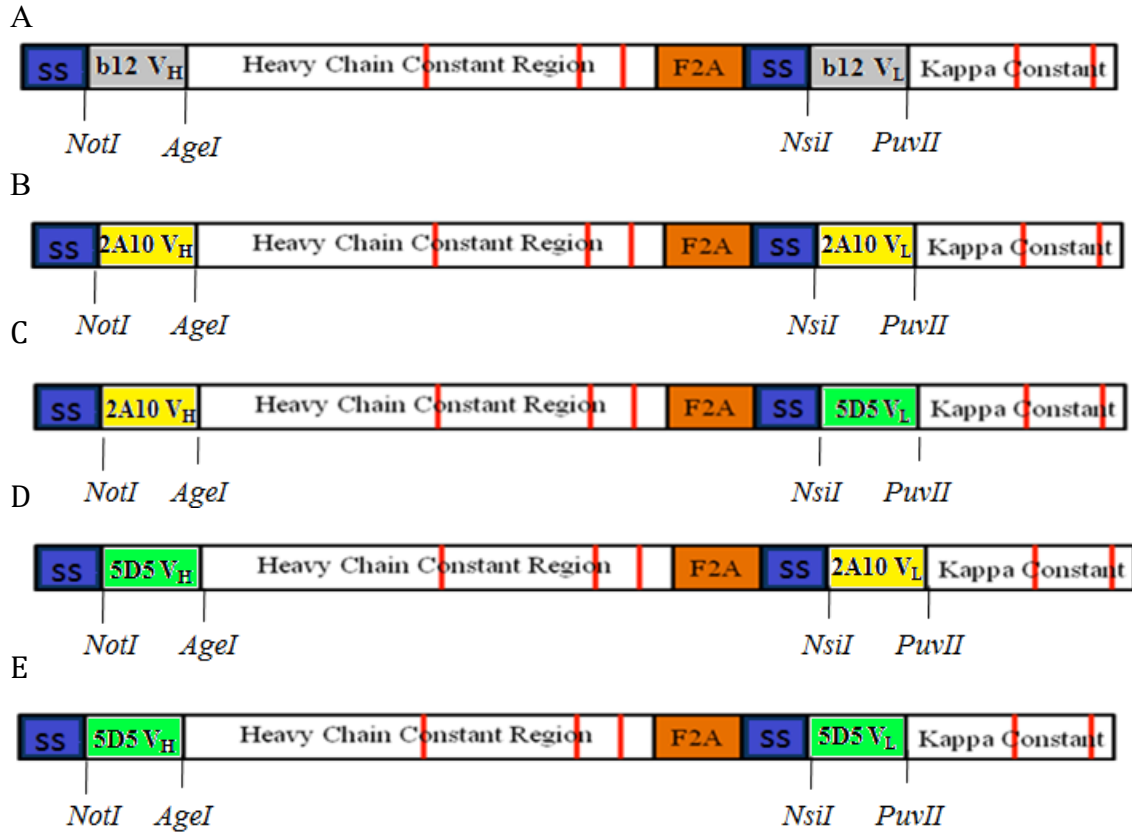


**Figure 5: Schematic representation of b12 transgene, 2A10 transgene, 5D5H-2A10 transgene, 5D5L-2A10 transgene and 5D5 transgene in VIP expression vector.**

A Transgene cassette in VIP expression vector containing b12 variable regions (grey boxes) called b12 VIP vector was prepared by David Baltimore's Laboratory. VIP vectors with this transgene express b12 monoclonal Antibody (mAb), an anti-HIV-1 mAb. (B) Transgene cassette in VIP expression vector containing 2A10 variable regions (yellow boxes) called 2A10 VIP vector was prepared by David Baltimore's Laboratory. VIP vectors with this transgene express 2A10 mAb that binds to the central repeat region of *P.falciparum* CSP<sup>36</sup>. (C) Transgene cassette in VIP expression vector containing 2A10 variable heavy (V<sub>H</sub>) chain (yellow box) and 5D5 variable light (V<sub>L</sub>) chain (green box) called 5D5L-2A10 VIP vector was prepared by replacing the 2A10 V<sub>L</sub> chain with 5D5 V<sub>L</sub> chain in 2A10 VIP vector. (D) Transgene cassette in VIP expression vector containing 5D5 V<sub>H</sub> chain (green box) and 2A10 V<sub>L</sub> chain (yellow box) called 5D5H-2A10

VIP vector was prepared by replacing the 2A10 V<sub>H</sub> chain with 5D5 V<sub>H</sub> chain in 2A10 VIP vector. Transgene cassette in VIP expression vector containing 5D5 variable regions (green boxes) called 5D5 VIP vector was prepared by replacing the 2A10 V<sub>L</sub> chain with 5D5 V<sub>L</sub> chain in 5D5H-2A10 VIP vector. VIP vectors with this transgene express 5D5 mAb that binds to N-terminus region near the proteolytic cleavage site of *P. falciparum* 3D7 CSP<sup>122</sup>.

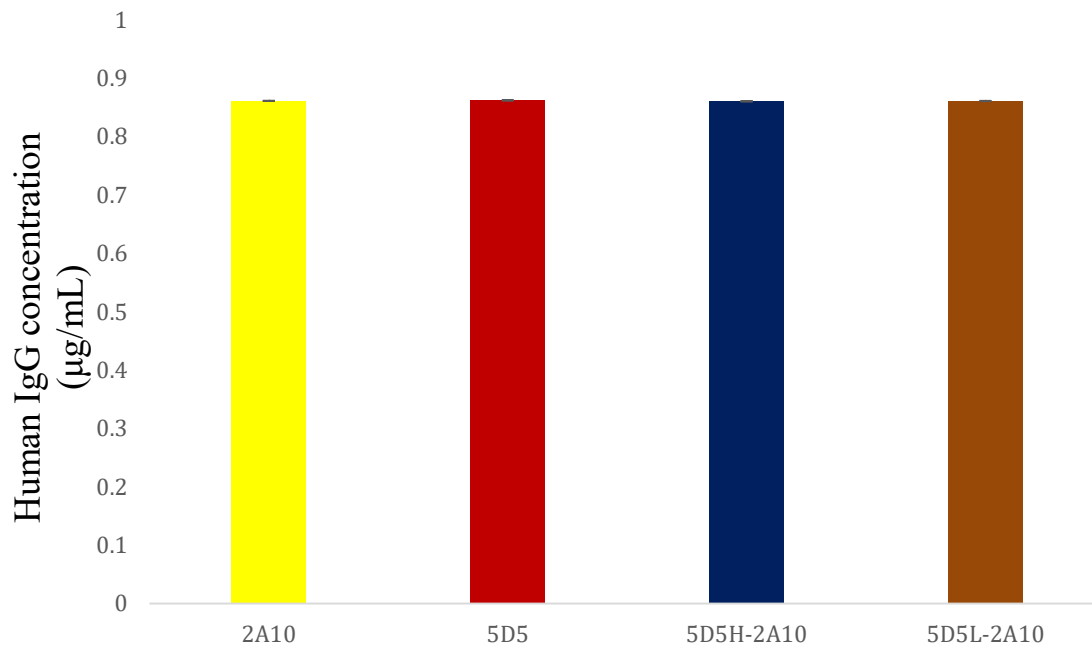


**Figure 6: Cloned VIP plasmids expressing high quantity of human IgG antibodies in vitro.**

The expression activity of each plasmid was tested in vitro by transfecting 293T cells with 2A10 VIP plasmid, 5D5 VIP plasmid, 5D5H-2A10 plasmid and 5D5L-2A10 plasmid. Supernatant from transfected cells was assayed for human IgG 48h post transfection by ELISA. The amount of the human IgG produced by the four plasmids was ~0.86 µg/mL.

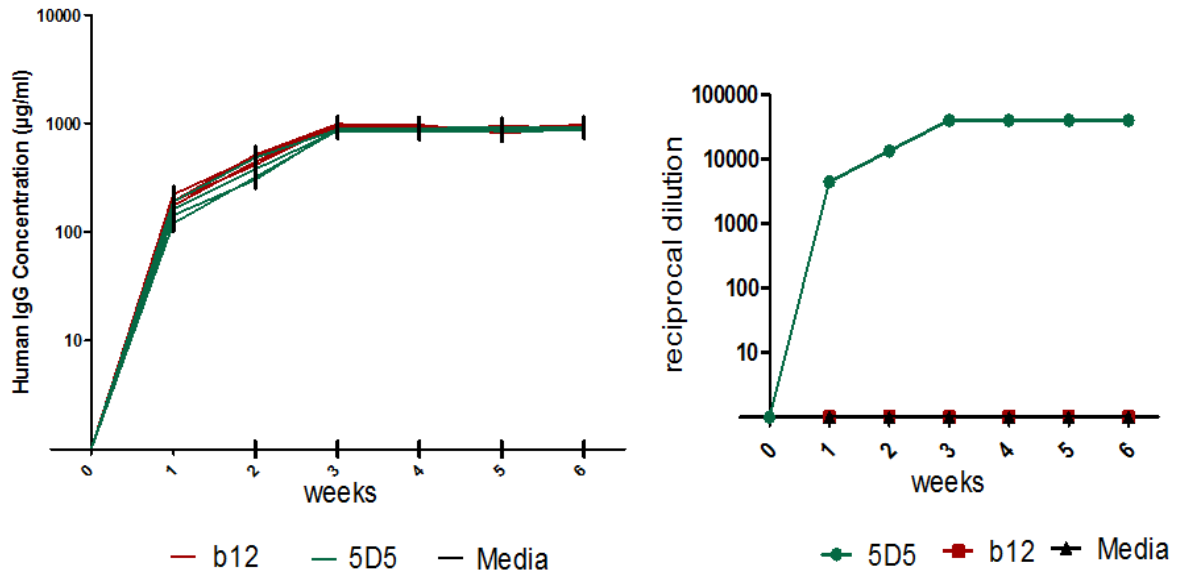


**Figure 7: 5D5-AAV8 expresses high levels of sustained human IgG antibody in vivo, and VIP- produced *Plasmodium falciparum* antibodies retain ability to recognize CSP.**

Quantification of human IgG (A) and anti-CSP antibodies (B) by ELISA after intramuscular injection of  $1 \times 10^{11}$  genome copies of the VIP expression vector producing b12 and 5D5 in female C57BL/6. The plot shows mean and standard error of titers for each mouse,  $n=4$  or 3 for media injected mice. All vectors express high levels of sustained human IgG antibody *in vivo*, and VIP- produced *Plasmodium falciparum* antibodies retain ability to recognize CSP.

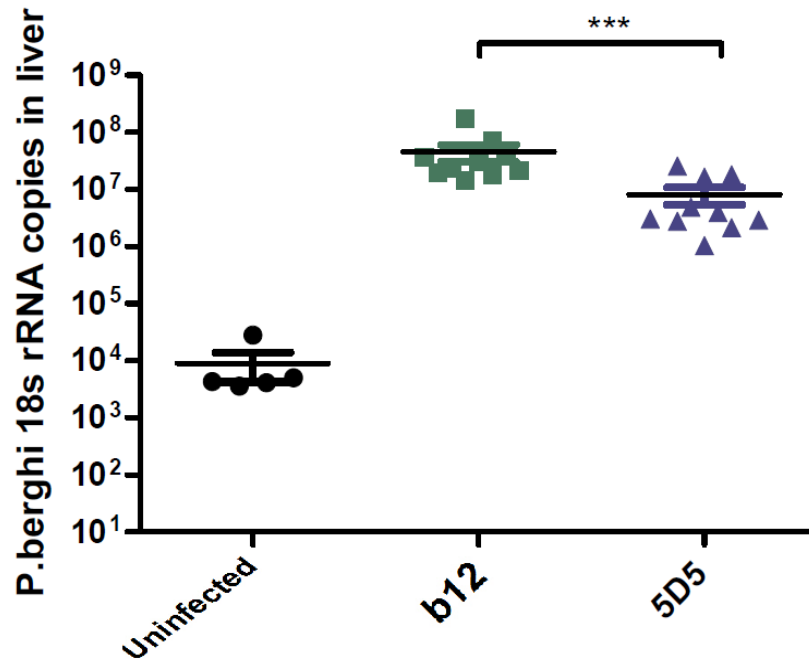


**Figure 8: VIP administration significantly reduces parasite burden in the liver.**

Six weeks post b12-AAV8 (anti-HIV-1 mAb expressing VIP system) and 5D5-AAV8 (anti-*P. falciparum* CSP mAb expressing VIP system) administration, mice were challenged

intravenously with  $1.0 \times 10^4$  *Pb-PfCSP* sporozoites. Mouse liver was extracted 38.5 hours post challenge and qPCR for *P. berghei* 18S rRNA copies was done to determine parasite burden.

The plot shows values for each individual mouse and the mean of the group (n=10 or 5 for uninfected). VIP administration significantly reduces parasite burden in the liver (\*\*\*) When p value  $\leq 0.001$ )

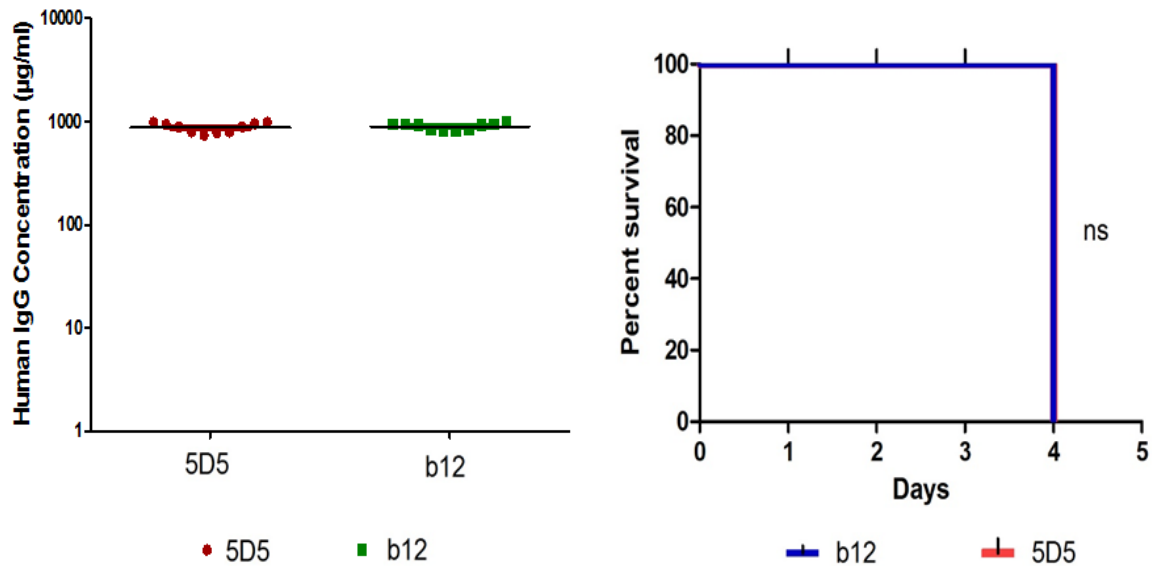


**Figure 9: VIP did not provide sterile protection to mice challenged by infected mosquito bite**

A) Concentration of human IgG in serum samples of mice transduced with 5D5-AAV and b12-AAV measured by ELISA, 6 weeks post transduction. Mice that received 5D5-AAV or b12-AAV challenged with *Pb-PfCSP* sporozoites delivered by infected mosquito bite, 6 weeks post-transduction. The Kaplan-Meier curve depicts percentage of mice that were parasite-free, determined by monitoring mice for the presence of blood-stage parasites in blood smears taken daily beginning at 4 days post challenge (n=10). 5D5-AAV transduced mice did not show delayed parasitemia compared to the b12-AAV group.

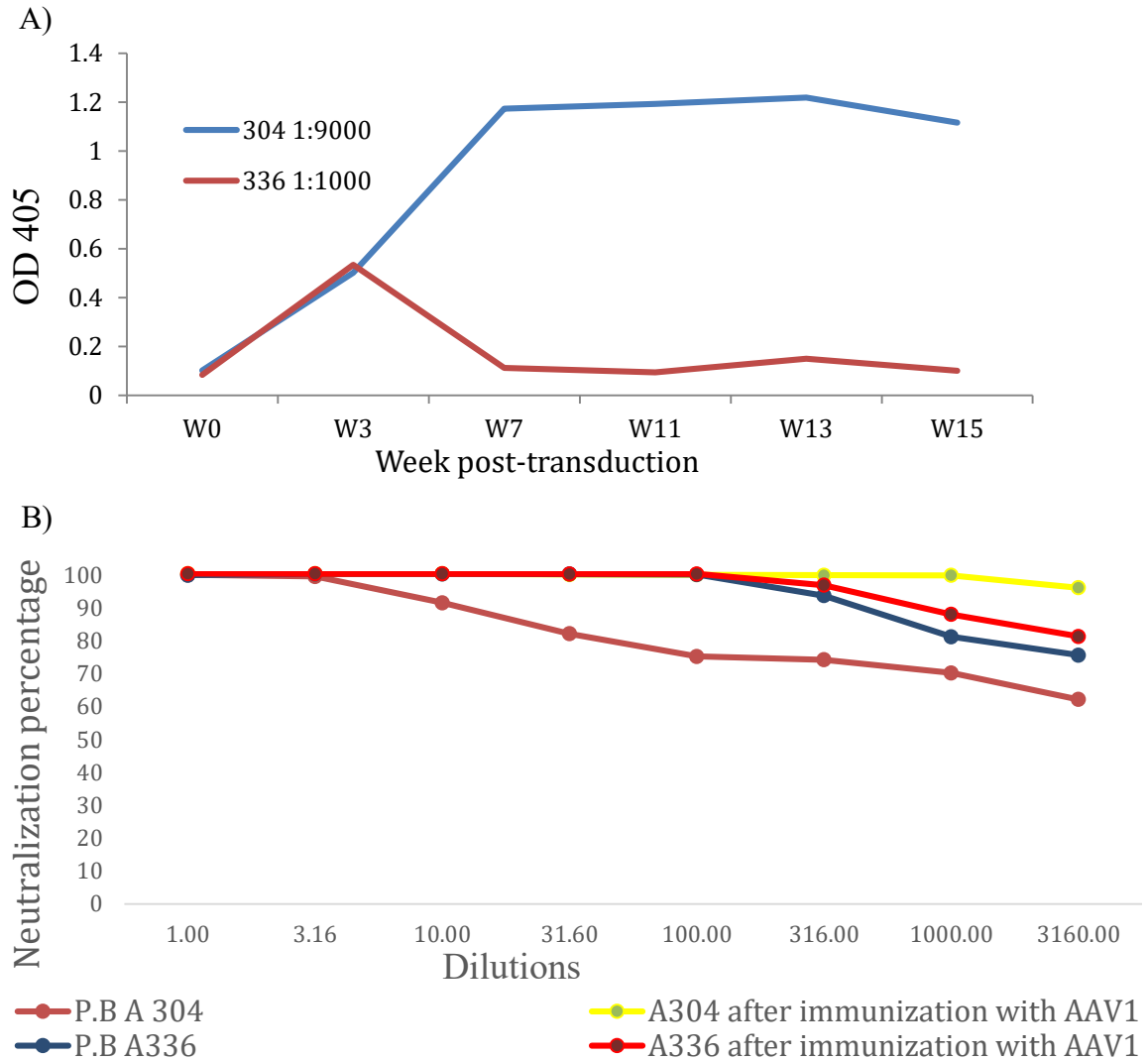


**Figure 10: Neutralizing antibody titers against AAV1 affect the expression of VIP in *Aotus* monkeys.**

(A) Anti-CSP antibodies present in the sera of Aotus monkey 304 and 336 transduced with AAV1 expressing 2A10 mAb was detected by ELISA, done by Dr. Gary Ketner. A304 expressed 2A10 mAb over 15 weeks post transduction, however A336 expressed 2A10 mAb until week three after which no anti- CSP antibody was detected. (B) Presence of neutralizing antibodies against the AAV1 in pre-bleed and after immunization with 2A10-AAV1 monkey sera was determined. A304 P.B that expressed 2A10 mAb had a lower titer of neutralizing antibodies compared to A336. After immunization the neutralizing antibodies titer in both monkeys



increased.

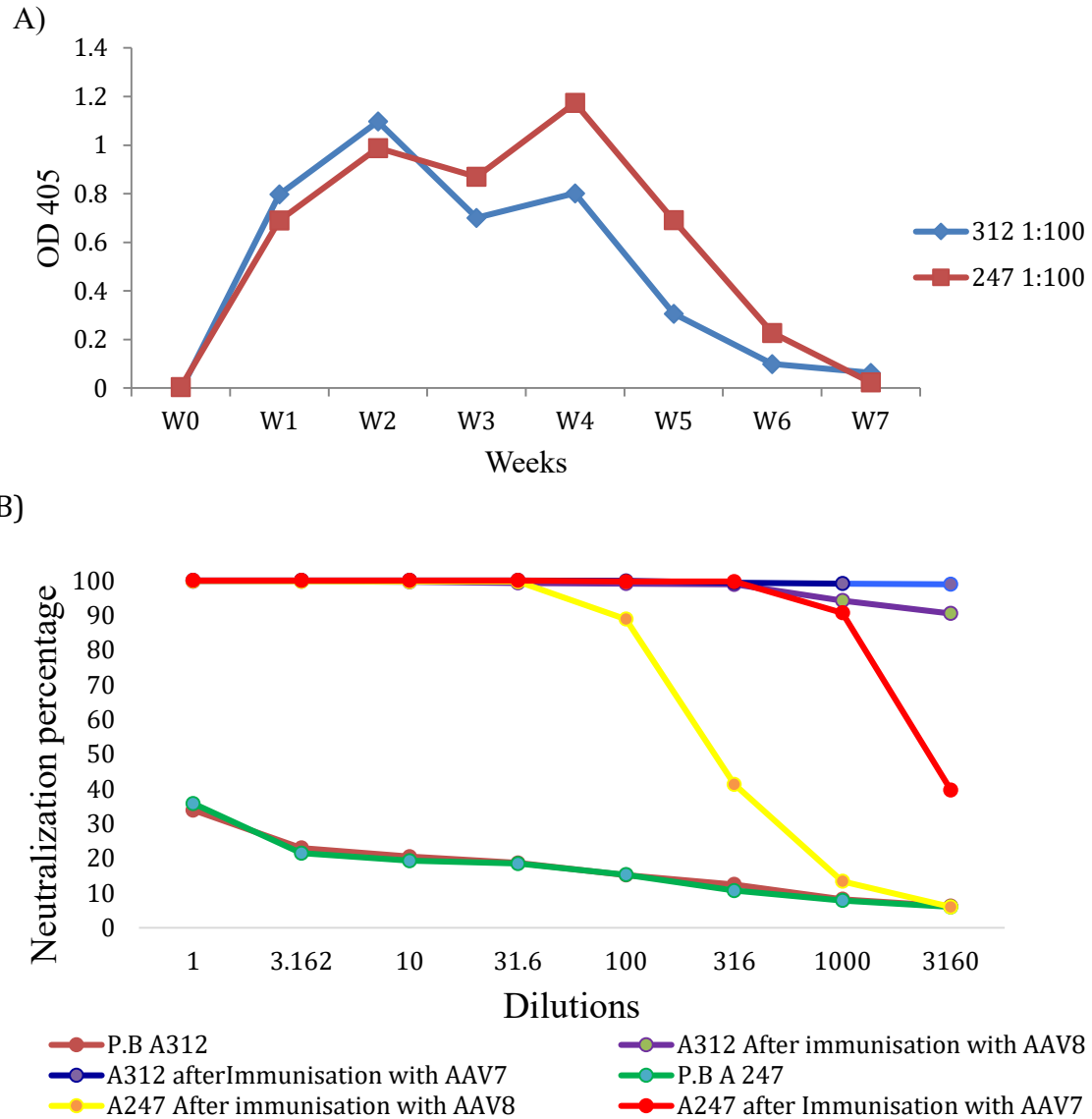


**Figure 11: VIP mAb expressed for a short period in *Aotus* monkeys having low neutralizing activity against AAV8.**

A) Anti-CSP antibodies present in the sera of *Aotus* monkey 312 and 247 transduced with AAV8 expressing 2A10 mAb was detected by ELISA, done by Dr. Gary Ketner. Both A312 and A247 expressed anti- CSP antibodies at varying amounts until no anti- CSP antibodies were detected 7 weeks post transduction) Presence of

neutralizing antibodies against AAV8 in pre-bleed, after immunization with 2A10-AAV8 and 2A10-AAV7 monkey sera were determined. Pre-bleeds of both monkeys had neutralizing activity (below 40%) that increased after immunization with 2A10-AAV8. The neutralizing activity against AAV8 monkeys increased further in both monkeys after immunization with 2A10-AAV7.

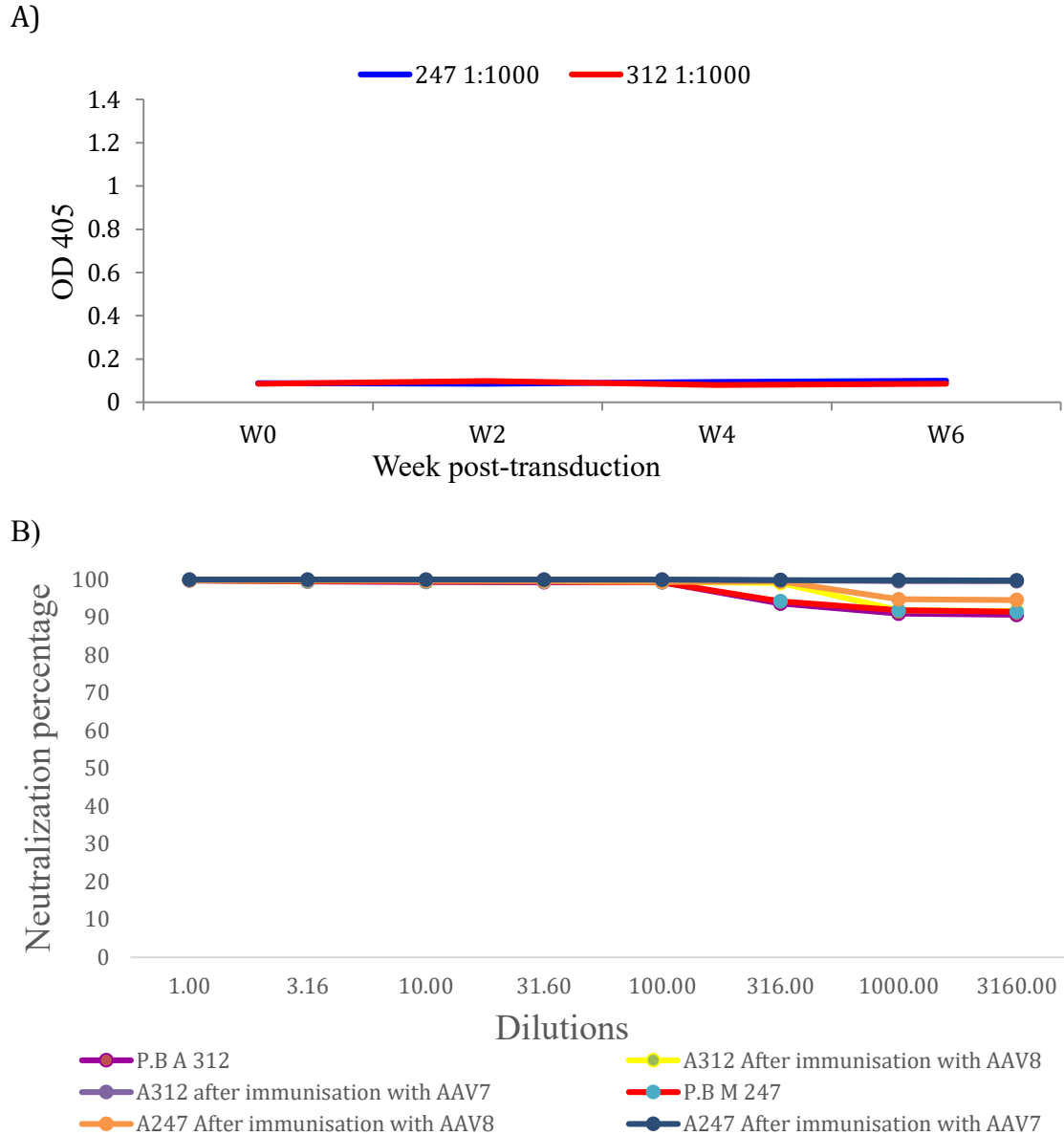


**Figure 12: High neutralization activity against AAV7 inhibits the expression of VIP mAb in Aotus monkeys.**

A) Anti-CSP antibodies present in the sera of *Aotus* monkey 312 and 336 transduced with 2A10-AAV7 expressing 2A10 mAb was detected by ELISA, done by Dr. Gary Ketner. Both A312 and A247 did not expressed any anti- CSP antibodies. B) Presence of neutralizing antibodies against AAV7 in pre-bleed, after immunization with 2A10-AAV8 and, after immunization with 2A10-

AAV7 monkey sera were determined. Pre-bleeds of both monkeys had high neutralizing activity (above 90%). Immunization with 2A10-AAV8 did not change the neutralizing percentage against AAV7 in both monkeys. The neutralizing activity against AAV7 increased after immunization with 2A10-AAV7.

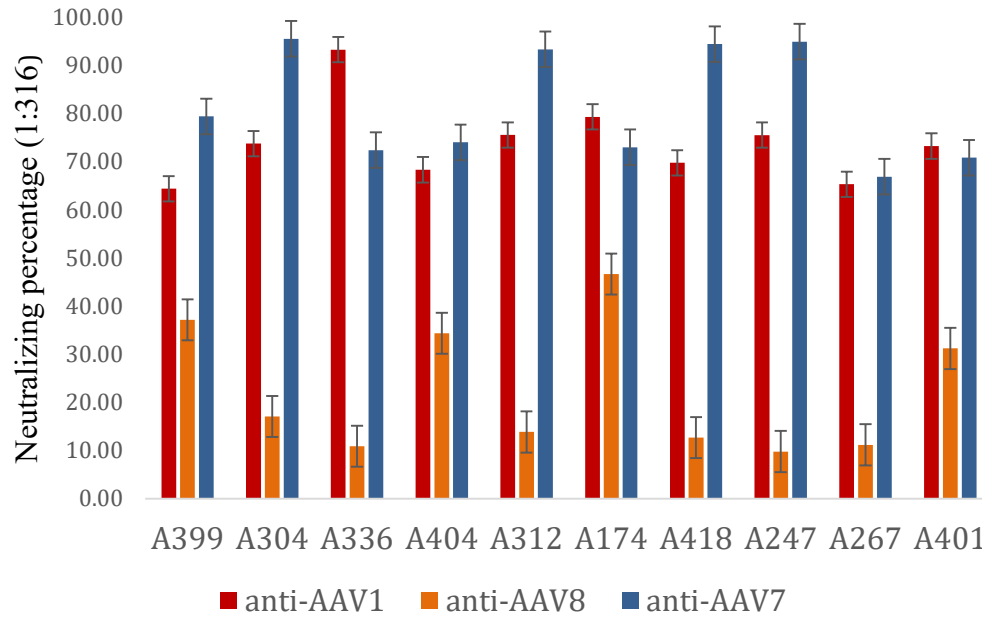


**Figure 13: Pre-screening of ten *Aotus* monkey sera for anti-AAV neutralizing antibodies against AAV1, -8 and -7.**

Pre-bleeds sera of ten *Aotus* monkeys were diluted to 1:316 and were screened for neutralizing antibodies against AAV1, -8 and -7. The cutoff neutralization value above which no VIP expression would occur was estimated to be 90% based on the 2A10-AAV1 neutralizing antibody experiments mentioned previously. Out of the ten monkeys, only A336 had a neutralizing activity above 90% against AAV1. All ten monkeys had neutralizing activity below 90% against AAV8. Four of the ten monkeys had neutralizing activity above 90% against AAV7 (A304, A312, A418 and A247). Pre-bleeds of ten *Aotus* monkeys were screened for neutralizing antibodies against AAV1. Only one monkey, A336 had a neutralizing activity above 90%.

## Discussion

Despite tremendous efforts, malaria remains a major global health problem with over 3.2 billion people still at risk from this parasitic disease<sup>1</sup>. The WHO estimates that there were 214 million cases of malaria in 2015 and 438,000 deaths<sup>1</sup>. The only malaria vaccine licensed is the RTS, S/AS01 which targets the human malarial parasite *P. falciparum*. RTS, S is a pre-erythrocytic malaria vaccine that consists of a hepatitis B surface antigen (HBsAg) fused to 19 copies of the central repeat region and C-terminal flanking region of *P. falciparum* incorporated into a virus-like particle with unfused HBsAg, which induces an immune response against CSP<sup>39</sup>. The vaccine efficacy of RTS, S was found to be below 50% and the protection it offers wanes over time<sup>42</sup>. Naturally acquired immunity develops in populations in areas where transmission is sustained but this immunity develops slowly and does not yield in sterile protection<sup>134</sup>. The only strategy that consistently provides sterile protection is vaccination with radiation-attenuated sporozoites, which is not clinically feasible in areas of high malaria burden as it requires bites by multiple infected irradiated mosquitoes or at least five intravenous injections with irradiated sporozoites<sup>19,28</sup>. Therefore, a different approach needs to be taken in the development of vaccines against malaria.

It has been known for a long time that antibodies targeting CSP can prevent malaria infection by inhibiting sporozoites from invading liver cells<sup>36,44</sup>. However for sterile protection, all sporozoites need to be neutralized before they reach the liver of the host. A single sporozoite successful in invading the liver can cause disease. David Baltimore's laboratory at California Institute of Technology developed a way to express high titer monoclonal human IgG antibodies *in vivo* by using an AAV vector, which is termed Vectored immunoprophylaxis (VIP). Humanized mice vaccinated using this approach were protected against HIV, and immune deficient mice were protected against a lethal influenza challenge, demonstrating the effectiveness of this technology in protecting against infectious diseases where antibody alone is protective<sup>120,121</sup>. Gary Ketner's

laboratory at Johns Hopkins Bloomberg School of public health characterized an AAV8 vector expressing humanized monoclonal anti-*P.falciparum* CSP antibodies 2A10 or 2C11. The mice that were transduced with 2A10-AAV and 2C11-AAV expressed high levels of human IgG, and these antibody levels were maintained over 52 weeks<sup>45</sup>. Mice expressing these mAbs showed a significant decrease in liver parasite burden after i.v tail vein challenge with transgenic *Pb/Pf P. berghei* parasites expressing CSP bearing the *P. falciparum* central repeat region<sup>45</sup>. 60% of 2A10-AAV and 30% of 2C11-AAV transduced mice showed sterile protection and the other mice in these groups showed delayed parasitemia compared to the control group when challenged by infected *Pb/Pf* mosquito bites<sup>45</sup>. The successful use of the VIP system against malaria has motivated further research to characterize other mAb expressing VIP systems.

5D5 is an anti- *P.falciparum* CSP monoclonal antibody that specifically binds to a linear epitope EDNEKLRKPKH in the N-terminus region of *P.falciparum* 3D7 CSP, inhibiting the CSP processing<sup>122</sup>, an essential process for the invasion of the liver by sporozoites while the previously characterized 2A10 mAb and 2C11 mAb bind to the central repeat region of *P.falciparum* CSP<sup>122</sup>. The 5D5 variable regions were cloned into the 2A10 VIP expression vector, replacing the 2A10 variable region sequences. Two intermediate VIP expression vectors, 5D5H-2A10 and 5D5L-2A10 were formed in the process. The amount of human immunoglobulin G (hIgG) produced by the 5D5 VIP plasmid and the intermediate plasmids were compared to the amount of hIgG produced by the original 2A10 VIP plasmid. All the plasmids produced similar amounts of human IgG (~0.86 µg/mL) indicating that the cloning of 5D5 variable chain sequences into the VIP plasmids did not affect the functionality of the plasmid. The functional 5D5 VIP plasmid was used to make an AAV8 vector virus expressing 5D5 mAb as previously described<sup>120</sup>.

*In vivo* studies of AAV8 expressing 5D5 in mice, resulted in mAb expression at ~100-1000 µg/mL of human IgG, as early as one week post transduction. The levels of human IgG

increased until 3 weeks post transduction and then was maintained at 800-1000 µg/mL until the end of the study (6 weeks). These levels of human IgG post VIP administration are similar to that produced by 2A10-AAV<sup>45</sup>. The expressed 5D5 mAbs recognized recombinant CSP which further supports the conclusion that manipulation and cloning of 5D5 sequence into the VIP plasmid did not affect the functionality of the mAb. Mice transduced with 5D5-AAV expressing hIgG levels between 700-1000 µg/mL showed a statistically significant reduction in liver parasite burden following i.v. *Pb/PfCSP* sporozoite challenge. The mice are sacrificed in this experiment 48h after i.v. *Pb/PfCSP* sporozoite challenge to extract their livers and delay to patency cannot be observed. When challenged by infected *Pb/PfCSP* mosquito bites, a more natural route of infection, no delay to patency and no sterile protection was observed in the 5D5 transduced mice expressing hIgG levels between 700-1000 µg/mL. This suggest that though 5D5 mAb effectively decreases the liver parasite burden, the decrease in liver parasite burden may not be sufficient to cause delay to patency in the mosquito bite challenge as the liver stage and the erythrocytic stage of the parasite are multiplication stage in the life cycle of the parasite. It is also of note that the use of synthetic humanized DNA sequences of the variable regions of the 5D5 mAb and the insertion of these variable region sequences into the VIP expression plasmid may have decreased the avidity of the 5D5 monoclonal antibody.

For sterile protection against *P.falciparum* infection, all mosquito inoculated sporozoites need to be neutralized before they invade the liver. This requires sustained high levels of mAb in the host which is possible by VIP system. Optimization of this vaccine may provide sterile protection. Optimization of this method includes the use of other pre-erythrocytic monoclonal antibodies with a greater protective capacity or the use of a combination of mAbs that target different binding sites in the CSP or bind to a completely different antigens in the pre-erythrocytic that may work synergistically to have a greater protective effect. While this particular study only utilized mAb targeting the N-terminus region of CSP, multiple stages of the parasite could easily be targeted at once via different mAb. The potential for this technology



is limitless and multiple approaches can be taken to optimize it as a form of malaria control. An obstacle to the use of AAV for therapeutics is the presence of pre-existing neutralizing anti-AAV antibodies and acquired antibodies generated after treatment with rAAVs that can reduce or inhibit the efficiency of these therapeutics, especially if the vector needs to administered repeatedly<sup>103,104</sup>. Around 30-80% of the world's population is estimated to be seropositive for antibodies against AAV serotypes 1 and 2, with anti-AAV2 being the most prevalent<sup>105</sup>. The development of this humoral response to AAV is thought to occur early in life around at the age of two as a consequence of WT AAV exposure<sup>108,109</sup>. Additionally, new born babies have been found to have maternal anti-AAV antibodies that decrease few months after birth but increase again<sup>108,109</sup>. These studies show that the time frame where individuals are naïve to Anti-AAV is narrow, making it difficult to administer AAV vectored therapeutics. In contrast to humans, AAV7, AAV8, AAV9, and AAVrh10 are the most seroprevalent AAV serotypes in non-human primates<sup>135-137</sup> and AAV2 has the lowest seroprevalence<sup>138</sup>. The prevalence of neutralizing anti-AAV antibodies in non-human primates puts forth a challenge to evaluate the performance of AAV vectored therapeutics.

In experiments to test the expression of 2A10 mAb by VIP in a non-human primate (NHP) that provides a *P. falciparum* challenge model, four *Aotus* monkeys - A304, A336, A312, and A247 were transduced with AAV vector expressing 2A10 mAb. A304 and A336 were transduced with 2A10-AAV1. A312 and A247 were transduced with 2A10-AAV8 and six months later they were transduced with 2A10-AAV7. The monkey sera were tested for anti-CSP antibody expression by ELISA, done by Dr. Gary Ketner. A304 transduced with 2A10-AAV1 expressed anti-CSP through the end of the experiment at fifteen weeks post transduction. The other monkey A336 showed brief anti- CSP antibody expression till week three after which the anti-CSP antibody expression declined until it was no longer detectable. Both A312 and A336 transduced with 2A10-AAV8 expressed anti-CSP antibodies for a brief time while A312 and A336 transduced

with 2A10-AAV7 six months after 2A10-AAV8 transduction did not express detectable levels of anti-CSP antibodies. From these results the vector that best expressed 2A10 by VIP was AAV1 (A304) in non-human primates. AAV8 failed to express AAV8 over long periods of time and AAV7 is extremely seroprevalent in non-human primates<sup>135–137</sup>.

By testing the pre-bleed sera of the monkeys (A304, A336, A312 and A247) for neutralizing anti-AAV antibodies, we concluded that pre-existing anti-AAV neutralizing antibodies may play a role in the effectiveness of AAV vectored mAb expression in the NPH models. In particular, in monkeys A304 and A336 transduced with 2A10-AAV1, higher neutralizing anti-AAV1 antibodies levels in A336 pre-bleed sera compared to A304 pre-bleed sera may account for the differences in AAV1-driven antibody synthesis. It was also noted anti-AAV1 antibody titer increased in both monkeys post 2A10-AAV1 administration which may pose a problem for the re-administration of the vaccine using the same vector in the same subjects. Similarly, the successful expression of anti-CSP antibodies few weeks after 2A10-AAV8 transduction in A312 and A247, may reflect the low titer of neutralizing anti-AAV8 antibodies in both monkey pre-bleeds and the titer of neutralizing anti-AAV8 antibodies increased post 2A10-AAV8 transduction and 2A10-AAV7 transduction. Pre-bleeds of A312 monkeys had high neutralizing activity against AAV7 which may explain that lack of 2A10 expression in these monkeys. Immunization with 2A10- AAV8 (6 months before 2A10-AAV7 transduction) did not change the neutralizing percentage against AAV7 in both monkeys. However, neutralizing activity against AAV7 increased in both monkeys post 2A10-AAV7 immunization.

Neutralizing anti-AAV antibodies do pose a major obstacle to the use of AAV as a vector for therapeutics but due to the extensive use and advantages of AAV as vector; many strategies have been developed to overcome this problem. This includes the pre-screening of subjects for pre-existing anti-AAV antibodies, development of novel, artificial AAV vectors<sup>113</sup>, plasmapheresis<sup>114</sup>, transient immunosuppression<sup>115,116</sup>, delivery of the vector with isolated perfusion and saline

flushing<sup>117</sup> and modulation of antibody responses with empty capsids<sup>118</sup>. Recently, a group of scientists used phylogenetic analysis to reconstruct an ancestral strain of AAV called Anc80L65. Anc80L65 is not neutralized by sera from mice immunized with several commonly-used AAV types<sup>139</sup>. Gene delivery through Anc80L65 has been shown to be successful in both mice and non-human primate models<sup>139</sup> and may prove to be a good vector for VIP method of vaccination.

Other immune responses like cytotoxic T lymphocyte responses against the vector may also effect the efficiency of transgene expression<sup>140</sup>. Studies have demonstrated that the activation of T cells against the vector capsid is limited to serotypes that have a heparin binding motif and exhibit heparin-binding activity<sup>141</sup>. Interestingly, serotypes such as AAV8 that lack this activity are better tolerated *in vivo* since they do not induce cytotoxic T lymphocyte responses, making it more likely that long term transduction will be achieved<sup>141</sup>. AAV vectored therapeutics administered at a low doses or into an immunoprivileged site have successfully expressed the transgene without the induction of a strong immune response against the vector<sup>142,143</sup>.

AAV vectors have been utilized for many years in both vaccine and gene therapy trials and have exhibited a good safety record. However, safety concerns still exist and a major concern centers on the ability of WT AAV to integrate into host DNA. *In vitro* studies have shown that WT AAV integrates in a site-specific manner on the chromosome 19q13.42 (AAVS1)<sup>79,80</sup>, chromosome 5p13.3 (AAVS2) and chromosome 3p24.3 (AAVS3)<sup>82</sup>. This site-specific integration of WT AAV in AAVS1 is *rep* dependent<sup>81</sup>, and *rep* is not present in rAAV used for gene therapy and other therapeutics. *In vivo* studies have shown the WT AAV DNA integrates at a low frequency and majority of the DNA exists as double stranded episomes in human tissue<sup>83</sup>. rAAV lacks many components of WT AAV but are still found to integrate into the host genome at a low frequency which can potentially lead to genotoxicity<sup>84</sup>. A recent study done to test the safety and site-specific integration of rAAV vectors using the EMA licensed AAV1-LPL<sup>S447X</sup> vector which was developed for the treatment of lipoprotein lipase deficiency (LPLD) showed that rAAV vector

integration was infrequent, mainly occurred within a nuclear mitochondrial DNA region (Similar sequences present in both mitochondrial and nuclear genomes<sup>86</sup>. The results also showed no significant vector genome integration in the AAVS1 locus or the AAV-HCC locus (implicated in AAV integration-mediated formation of hepatocellular carcinoma)<sup>86</sup>, further supporting the safety of rAAV and their use as a vector for therapeutics and vaccination strategies.

Despite decades of research, the only malaria vaccine to be licensed is RTS, S/AS01. This vaccine cannot be used in the fight to eradicate malaria as it has a low efficacy and does not protect for a long period of time<sup>42</sup>. Research is ongoing to develop second-generation vaccines. Given the disease burden caused by malaria and the importance of eradicating it, novel vaccine approaches need to be explored as well. Our work demonstrates the feasibility of using a viral vector to express broadly neutralizing antibodies against malaria at high titers for a sustained period of time. With optimization of this strategy, VIP could be used in endemic areas as immunization strategy with the end goal of eradication.

## References

1. WHO | Malaria. *WHO*. 2016.
2. Snow RW, Omumbo JA. *Malaria*.; 2006. <http://www.ncbi.nlm.nih.gov/pubmed/21290647>. Accessed March 15, 2016.
3. Payne D. Spread of chloroquine resistance in *Plasmodium falciparum*. *Parasitol Today*. 1987;3(8):241-246. doi:10.1016/0169-4758(87)90147-5.
4. Noedl H, Se Y, Schaecher K, Smith BL, Socheat D, Fukuda MM. Evidence of Artemisinin-resistant malaria in Western Cambodia. *N Engl J Med*. 2008;359(24):2619-2620. doi:10.1056/NEJMc0805011.
5. Dondorp AM, Nosten F, Yi P, et al. Artemisinin resistance in *Plasmodium falciparum* malaria. *N Engl J Med*. 2009;361(5):455-467. doi:10.1056/NEJMoa0808859.
6. Warrel DA, Gilles HM. *Essential Malariology*. 4th ed. (D. A. Warrell HMG, ed.). Arnold; 2002.
7. Waters AP, Janse CJ. *Malaria Parasites. Genomes and Molecular Biology*. Caister Academic Press; 2004.
8. Amino R, Thiberge S, Blazquez S, et al. Imaging malaria sporozoites in the dermis of the mammalian host. *Nat Protoc*. 2007;2(7):1705-1712. doi:10.1038/nprot.2007.120.
9. Hillyer JF, Barreau C, Vernick KD. Efficiency of salivary gland invasion by malaria sporozoites is controlled by rapid sporozoite destruction in the mosquito haemocoel. *Int J Parasitol*. 2007;37(6):673-681. doi:10.1016/j.ijpara.2006.12.007.

10. Fujioka H, Aikawa M. Structure and Life Cycle. In: *Malaria Immunology*. Basel: KARGER; 2002:1-26. doi:10.1159/000058837.
11. Amino R, Thiberge S, Martin B, et al. Quantitative imaging of Plasmodium transmission from mosquito to mammal. *Nat Med*. 2006;12(2):220-224. doi:10.1038/nm1350.
12. Yuda M, Ishino T. Liver invasion by malarial parasites--how do malarial parasites break through the host barrier? *Cell Microbiol*. 2004;6(12):1119-1125. doi:10.1111/j.1462-5822.2004.00474.x.
13. Crutcher JM, Hoffman SL. *Malaria*.; 1996.  
<http://www.ncbi.nlm.nih.gov/pubmed/21413352>. Accessed March 15, 2016.
14. Kantele A, Jokiranta S. [Plasmodium knowlesi--the fifth species causing human malaria]. *Duodecim*. 2010;126(4):427-434. <http://www.ncbi.nlm.nih.gov/pubmed/20486493>.
15. McQueen PG, McKenzie FE. Competition for red blood cells can enhance Plasmodium vivax parasitemia in mixed-species malaria infections. *Am J Trop Med Hyg*. 2006;75(1):112-125. doi:75/1/112 [pii].
16. Vaughan AM, Kappe SHI. Malaria vaccine development: Persistent challenges. *Curr Opin Immunol*. 2012;24(3):324-331. doi:10.1016/j.coi.2012.03.009.
17. Weiss WR, Jiang CG. Protective CD8+ T lymphocytes in primates immunized with malaria sporozoites. *PLoS One*. 2012;7(2). doi:10.1371/journal.pone.0031247.
18. Weiss WR, Sedegah M, Beaudoin RL, Miller LH, Good MF. CD8+ T cells (cytotoxic/suppressors) are required for protection in mice immunized with malaria sporozoites. *Proc Natl Acad Sci U S A*. 1988;85:573-576. doi:10.1073/pnas.85.2.573.

19. Hoffman SL, Goh LML, Luke TC, et al. Protection of humans against malaria by immunization with radiation-attenuated *Plasmodium falciparum* sporozoites. *J Infect Dis.* 2002;185(8):1155-1164. doi:10.1086/339409.
20. Jin Y, Kebaier C, Vanderberg J. Direct microscopic quantification of dynamics of *Plasmodium berghei* sporozoite transmission from mosquitoes to mice. *Infect Immun.* 2007;75(11):5532-5539. doi:10.1128/IAI.00600-07.
21. Medica DL, Sinnis P. Quantitative dynamics of *Plasmodium yoelii* sporozoite transmission by infected anopheline mosquitoes. *Infect Immun.* 2005;73(7):4363-4369. doi:10.1128/IAI.73.7.4363-4369.2005.
22. Sultan AA, Thathy V, Frevert U, et al. TRAP is necessary for gliding motility and infectivity of *Plasmodium* sporozoites. *Cell.* 1997;90(3):511-522. doi:10.1016/S0092-8674(00)80511-5.
23. Baldacci P, Ménard R. The elusive malaria sporozoite in the mammalian host. *Mol Microbiol.* 2004;54(2):298-306. doi:10.1111/j.1365-2958.2004.04275.x.
24. Fidock DA, Gras-Masse H, Lepers JP, et al. *Plasmodium falciparum* liver stage antigen-1 is well conserved and contains potent B and T cell determinants. *J Immunol.* 1994;153(1):190-204. <http://www.ncbi.nlm.nih.gov/pubmed/7515922>.
25. Duffy PE, Sahu T, Akue A, Milman N, Anderson C. Pre-erythrocytic malaria vaccines: identifying the targets. *Expert Rev Vaccines.* 2012;11(10):1261-1280. doi:10.1586/erv.12.92.
26. Nussenzweig RS, Vanderberg J, Most H, Orton C. Protective immunity produced by the injection of x-irradiated sporozoites of *plasmodium berghei*. *Nature.* 1967;216(5111):160-162. doi:10.1038/216160a0.

27. Gwadz RW, Cochrane AH, Nussenzweig V, Nussenzweig RS. Preliminary studies on vaccination of rhesus monkeys with irradiated sporozoites of *Plasmodium knowlesi* and characterization of surface antigens of these parasites. *Bull World Health Organ.* 1979;57(Suppl. 1):165-173.
28. Seder RA, Chang L-J, Enama ME, et al. Protection against malaria by intravenous immunization with a nonreplicating sporozoite vaccine. *Science.* 2013;341(6152):1359-1365. doi:10.1126/science.1241800.
29. Kumar KA, Sano G, Boscardin S, et al. The circumsporozoite protein is an immunodominant protective antigen in irradiated sporozoites. *Nature.* 2006;444(7121):937-940. doi:10.1038/nature05361.
30. Tewari R, Spaccapelo R, Bistoni F, Holder AA, Crisanti A. Function of region I and II adhesive motifs of *Plasmodium falciparum* circumsporozoite protein in sporozoite motility and infectivity. *J Biol Chem.* 2002;277(49):47613-47618. doi:10.1074/jbc.M208453200.
31. Singh AP, Buscaglia CA, Wang Q, et al. *Plasmodium* Circumsporozoite Protein Promotes the Development of the Liver Stages of the Parasite. *Cell.* 2007;131(3):492-504. doi:10.1016/j.cell.2007.09.013.
32. Sidjanski SP, Vanderberg JP, Sinnis P. Anopheles stephensi salivary glands bear receptors for region I of the circumsporozoite protein of *Plasmodium falciparum*. *Mol Biochem Parasitol.* 1997;90(1):33-41. doi:10.1016/S0166-6851(97)00124-2.
33. Ménard R, Sultan a a, Cortes C, et al. Circumsporozoite protein is required for development of malaria sporozoites in mosquitoes. *Nature.* 1997;385(6614):336-340. doi:10.1038/385336a0.



34. Zavala F, Cochrane AH, Nardin EH, Nussenzweig RS, Nussenzweig V. Circumsporozoite proteins of malaria parasites contain a single immunodominant region with two or more identical epitopes. *J Exp Med.* 1983;157(6):1947-1957. doi:10.1084/jem.157.6.1947.
35. Zavala F, Masuda A, Graves PM, Nussenzweig V, Nussenzweig RS. Ubiquity of the repetitive epitope of the CS protein in different isolates of human malaria parasites. *J Immunol.* 1985;135(0022-1767 (Print)):2790-2793.
36. Zavala F, Tam JP, Hollingdale MR, et al. Rationale for development of a synthetic vaccine against Plasmodium falciparum malaria. *Sci (New York, NY).* 1985;228(4706):1436-1440. doi:10.1126/science.2409595.
37. Yamauchi Lucy M. LM, Coppi A, Snounou G, Sinnis P. Plasmodium sporozoites trickle out of the injection site. *Cell Microbiol.* 2007;9(5):1215-1222. doi:10.1111/j.1462-5822.2006.00861.x.
38. European Medicines Agency. First malaria vaccine receives positive scientific opinion from EMA. *Press release.* 2015;44(July):1-3.  
[http://www.ema.europa.eu/docs/en\\_GB/document\\_library/Press\\_release/2015/07/WC500190447.pdf](http://www.ema.europa.eu/docs/en_GB/document_library/Press_release/2015/07/WC500190447.pdf).
39. Heppner DG, Kester KE, Ockenhouse CF, et al. Towards an RTS,S-based, multi-stage, multi-antigen vaccine against falciparum malaria: Progress at the Walter Reed Army Institute of Research. In: *Vaccine.* Vol 23. ; 2005:2243-2250.  
doi:10.1016/j.vaccine.2005.01.142.
40. Stoute J a, Slaoui M, Heppner DG, et al. A preliminary evaluation of a recombinant circumsporozoite protein vaccine against Plasmodium falciparum malaria. RTS,S Malaria

- Vaccine Evaluation Group. *N Engl J Med*. 1997;336(2):86-91.  
doi:10.1056/NEJM199701093360202.
41. Gordon DM, McGovern TW, Krzych U, et al. Safety, immunogenicity, and efficacy of a recombinantly produced *Plasmodium falciparum* circumsporozoite protein-hepatitis B surface antigen subunit vaccine. *J Infect Dis*. 1995;171(6):1576-1585.  
doi:10.1093/infdis/171.6.1576.
  42. Partnership SCT. Efficacy and safety of the RTS,S/AS01 malaria vaccine during 18 months after vaccination: a phase 3 randomized, controlled trial in children and young infants at 11 African sites. *PLoS Med*. 2014;11(7):e1001685.  
doi:10.1371/journal.pmed.1001685.
  43. Efficacy and safety of RTS,S/AS01 malaria vaccine with or without a booster dose in infants and children in Africa: final results of a phase 3, individually randomised, controlled trial. *Lancet*. 2015;386(9988):31-45. doi:10.1016/S0140-6736(15)60721-8.
  44. Nardin EH, Nussenzweig V, Nussenzweig RS, et al. Circumsporozoite proteins of human malaria parasites *Plasmodium falciparum* and *Plasmodium vivax*. *J Exp Med*. 1982;156(1):20-30. doi:10.1084/jem.156.1.20.
  45. Deal C, Balazs AB, Espinosa DA, Zavala F, Baltimore D, Ketner G. Vectored antibody gene delivery protects against *Plasmodium falciparum* sporozoite challenge in mice. *Proc Natl Acad Sci U S A*. 2014;111(34):12528-12532. doi:10.1073/pnas.1407362111.
  46. Xie Q, Bu W, Bhatia S, et al. The atomic structure of adeno-associated virus (AAV-2), a vector for human gene therapy. *Proc Natl Acad Sci U S A*. 2002;99(16):10405-10410.  
doi:10.1073/pnas.162250899.

47. Govindasamy L, Padron E, McKenna R, et al. Structurally mapping the diverse phenotype of adeno-associated virus serotype 4. *J Virol.* 2006;80(23):11556-11570. doi:10.1128/JVI.01536-06.
48. Nam H-J, Lane MD, Padron E, et al. Structure of adeno-associated virus serotype 8, a gene therapy vector. *J Virol.* 2007;81(22):12260-12271. doi:10.1128/JVI.01304-07.
49. Lerch TF, Xie Q, Chapman MS. The structure of adeno-associated virus serotype 3B (AAV-3B): Insights into receptor binding and immune evasion. *Virology.* 2010;403(1):26-36. doi:10.1016/j.virol.2010.03.027.
50. DiMattia M a, Nam H-J, Van Vliet K, et al. Structural insight into the unique properties of adeno-associated virus serotype 9. *J Virol.* 2012;86(12):6947-6958. doi:10.1128/JVI.07232-11.
51. Srivastava A, Lusby EW, Berns KI. Nucleotide sequence and organization of the adeno-associated virus 2 genome. *J Virol.* 1983;45(2):555-564.   
<http://www.pubmedcentral.nih.gov/articlerender.fcgi?artid=256449&tool=pmcentrez&rendertype=abstract>.
52. McLaughlin SK, Collis P, Hermonat PL, Muzyczka N. Adeno-associated virus general transduction vectors: analysis of proviral structures. *J Virol.* 1988;62(6):1963-1973.   
<http://www.pubmedcentral.nih.gov/articlerender.fcgi?artid=253280&tool=pmcentrez&rendertype=abstract>.
53. Nonnenmacher M, Weber T. Intracellular transport of recombinant adeno-associated virus vectors. *Gene Ther.* 2012;19(6):649-658. doi:10.1038/gt.2012.6.

54. Pereira DJ, McCarty DM, Muzyczka N. The adeno-associated virus (AAV) Rep protein acts as both a repressor and an activator to regulate AAV transcription during a productive infection. *J Virol.* 1997;71(2):1079-1088.
55. Labow M a, Hermonat PL, Berns KI. Positive and negative autoregulation of the adeno-associated virus type 2 genome. *J Virol.* 1986;60(1):251-258.  
<http://www.pubmedcentral.nih.gov/articlerender.fcgi?artid=253923&tool=pmcentrez&rendertype=abstract>.
56. Kyöstiö SR, Owens RA, Weitzman MD, Antoni BA, Chejanovsky N, Carter BJ. Analysis of adeno-associated virus (AAV) wild-type and mutant Rep proteins for their abilities to negatively regulate AAV p5 and p19 mRNA levels. *J Virol.* 1994;68(5):2947-2957.  
<http://www.pubmedcentral.nih.gov/articlerender.fcgi?artid=236783&tool=pmcentrez&rendertype=abstract>.
57. Hölscher C, Kleinschmidt J a, Bürkle a. High-level expression of adeno-associated virus (AAV) Rep78 or Rep68 protein is sufficient for infectious-particle formation by a rep-negative AAV mutant. *J Virol.* 1995;69(11):6880-6885.  
<http://www.pubmedcentral.nih.gov/articlerender.fcgi?artid=189603&tool=pmcentrez&rendertype=abstract>.
58. Lackner DF, Muzyczka N. Studies of the mechanism of transactivation of the adeno-associated virus p19 promoter by Rep protein. *J Virol.* 2002;76(16):8225-8235.  
doi:10.1128/JVI.76.16.8225-8235.2002.
59. Labow MA, Graf Jr. LH, Berns KI. Adeno-associated virus gene expression inhibits cellular transformation by heterologous genes. *Mol Cell Biol.* 1987;7(4):1320-1325.  
[http://www.ncbi.nlm.nih.gov/entrez/query.fcgi?cmd=Retrieve&db=PubMed&dopt=Citation&list\\_uids=3037312](http://www.ncbi.nlm.nih.gov/entrez/query.fcgi?cmd=Retrieve&db=PubMed&dopt=Citation&list_uids=3037312).

60. McCarty DM, Christensen M, Muzyczka N. Sequences required for coordinate induction of adeno-associated virus p19 and p40 promoters by Rep protein. *J Virol.* 1991;65(6):2936-2945.  
<http://www.pubmedcentral.nih.gov/articlerender.fcgi?artid=240929&tool=pmcentrez&rendertype=abstract>.
61. King JA, Dubielzig R, Grimm D, Kleinschmidt JA. DNA helicase-mediated packaging of adeno-associated virus type 2 genomes into preformed capsids. *EMBO J.* 2001;20(12):3282-3291. doi:10.1093/emboj/20.12.3282.
62. Hickman AB, Ronning DR, Kotin RM, Dyda F. Structural unity among viral origin binding proteins: Crystal structure of the nuclease domain of adeno-associated virus Rep. *Mol Cell.* 2002;10(2):327-337. doi:10.1016/S1097-2765(02)00592-0.
63. Im DS, Muzyczka N. The AAV origin binding protein Rep68 is an ATP-dependent site-specific endonuclease with DNA helicase activity. *Cell.* 1990;61(3):447-457. doi:10.1016/0092-8674(90)90526-K.
64. Agbandje-McKenna M, Kleinschmidt J. AAV capsid structure and cell interactions. *Methods Mol Biol.* 2011;807:47-92. doi:10.1007/978-1-61779-370-7\_3.
65. Qing K, Mah C, Hansen J, Zhou S, Dwarki V, Srivastava A. Human fibroblast growth factor receptor 1 is a co-receptor for infection by adeno-associated virus 2. *Nat Med.* 1999;5(1):71-77. doi:10.1038/4758.
66. Akache B, Grimm D, Pandey K, Yant SR, Xu H, Kay M a. The 37/67-kilodalton laminin receptor is a receptor for adeno-associated virus serotypes 8, 2, 3, and 9. *J Virol.* 2006;80(19):9831-9836. doi:10.1128/JVI.00878-06.

67. Ummerford CAS, Artlett JESB, Amulski RIJUDES.  $\alpha V\beta 5$  integrin : a co-receptor for adeno-associated virus type 2 infection. *Nat Med.* 1999;5(1):1-5.
68. Bartlett JS, Wilcher R, Samulski RJ. Infectious entry pathway of adeno-associated virus and adeno-associated virus vectors. *J Virol.* 2000;74(6):2777-2785.  
doi:10.1128/JVI.74.6.2777-2785.2000.
69. Weitzman MD, Linden RM. Adeno-associated virus biology. *Methods Mol Biol.* 2011;807:1-23. doi:10.1007/978-1-61779-370-7\_1.
70. Trempe JP, Carter BJ. Regulation of adeno-associated virus gene expression in 293 cells: control of mRNA abundance and translation. *J Virol.* 1988;62(1):68-74.  
<http://www.pubmedcentral.nih.gov/articlerender.fcgi?artid=250502&tool=pmcentrez&rendertype=abstract>.
71. Redemann BE, Mendelson E, Carter BJ. Adeno-associated virus rep protein synthesis during productive infection. *J Virol.* 1989;63(2):873-882.
72. Senapathy P, Tratschin JD, Carter BJ. Replication of adeno-associated virus DNA. Complementation of naturally occurring rep- mutants by a wild-type genome or an fori-mutant and correction of terminal palindrome deletions. *J Mol Biol.* 1984;179(1):1-20.  
doi:10.1016/0022-2836(84)90303-6.
73. Nahreini P, Srivastava A. Rescue and replication of the adeno-associated virus 2 genome in mortal and immortal human cells. *Intervirology.* 1989;30(2):74-85.  
<http://www.ncbi.nlm.nih.gov/pubmed/2542184>.
74. Nash K, Chen W, Muzyczka N. Complete in vitro reconstitution of adeno-associated virus DNA replication requires the minichromosome maintenance complex proteins. *J Virol.* 2008;82(3):1458-1464. doi:10.1128/JVI.01968-07.

75. Slanina H, Weger S, Stow ND, Kuhrs A, Heilbronn R. Role of the herpes simplex virus helicase-primase complex during adeno-associated virus DNA replication. *J Virol.* 2006;80(11):5241-5250.  
[http://www.ncbi.nlm.nih.gov/entrez/query.fcgi?cmd=Retrieve&db=PubMed&dopt=Citation&list\\_uids=16699004](http://www.ncbi.nlm.nih.gov/entrez/query.fcgi?cmd=Retrieve&db=PubMed&dopt=Citation&list_uids=16699004).
76. Ward P, Falkenberg M, Elias P, Weitzman M, Linden RM. Rep-dependent initiation of adeno-associated virus type 2 DNA replication by a herpes simplex virus type 1 replication complex in a reconstituted system. *J Virol.* 2001;75(21):10250-10258. doi:10.1128/JVI.75.21.10250-10258.2001.
77. Brister JR, Muzyczka N. Mechanism of Rep-mediated adeno-associated virus origin nicking. *J Virol.* 2000;74(17):7762-7771. doi:10.1128/JVI.74.17.7762-7771.2000.Updated.
78. Ward P, Elias P, Linden RM. Rescue of the adeno-associated virus genome from a plasmid vector: evidence for rescue by replication. *J Virol.* 2003;77(21):11480-11490. <http://www.ncbi.nlm.nih.gov/pubmed/14557633>. Accessed March 15, 2016.
79. Kotin RM, Berns KI. Organization of adeno-associated virus DNA in latently infected detroit 6 cells. *Virology.* 1989;170(2):460-467. doi:10.1016/0042-6822(89)90437-6.
80. Kotin RM, Menninger JC, Ward DC, Berns KI. Mapping and direct visualization of a region-specific viral DNA integration site on chromosome 19q13-qter. *Genomics.* 1991;10(3):831-834. doi:10.1016/0888-7543(91)90470-Y.
81. Miller JL, Donahue RE, Sellers SE, Samulski RJ, Young NS, Nienhuis AW. Recombinant adeno-associated virus (rAAV)-mediated expression of a human gamma-globin gene in human progenitor-derived erythroid cells. *Proc Natl Acad Sci U S A.* 1994;91(21):10183-10187.

<http://www.pubmedcentral.nih.gov/articlerender.fcgi?artid=44982&tool=pmcentrez&rendertype=abstract>.

82. Hüser D, Gogol-Döring A, Lutter T, et al. Integration preferences of wildtype AAV-2 for consensus rep-binding sites at numerous loci in the human genome. *PLoS Pathog.* 2010;6(7):1-14. doi:10.1371/journal.ppat.1000985.
83. Schnepf BC, Jensen RL, Chen CL, Johnson PR, Clark KR. Characterization of adeno-associated virus genomes isolated from human tissues. *J Virol.* 2005;79(23):14793-14803. doi:10.1128/JVI.79.23.14793-14803.2005.
84. Donsante a, Vogler C, Muzyczka N, et al. Observed incidence of tumorigenesis in long-term rodent studies of rAAV vectors. *Gene Ther.* 2001;8(17):1343-1346. doi:10.1038/sj.gt.3301541.
85. Deyle DR, Russell DW. Adeno-associated virus vector integration. *Curr Opin Mol Ther.* 2009;11(4):442-447.  
<http://www.pubmedcentral.nih.gov/articlerender.fcgi?artid=2929125&tool=pmcentrez&rendertype=abstract>.
86. Kaepfel C, Beattie SG, Fronza R, et al. A largely random AAV integration profile after LPLD gene therapy. *Nat Med.* 2013;19(7):889-891. doi:10.1038/nm.3230.
87. ATCHISON RW, CASTO BC, HAMMON WM. ADENOVIRUS-ASSOCIATED DEFECTIVE VIRUS PARTICLES. *Science.* 1965;149(3685):754-756. doi:10.1126/science.149.3685.754.
88. Daya S, Berns KI. Gene therapy using adeno-associated virus vectors. *Clin Microbiol Rev.* 2008;21(4):583-593. doi:10.1128/CMR.00008-08.



89. Hastie E, Samulski RJ. AAV at 50: A golden anniversary of discovery, research, and gene therapy success, a personal perspective. *Hum Gene Ther*. 2015;265(May):1-24. doi:10.1089/hum.2015.025.
90. Jacobson SG, Cideciyan A V., Roman AJ, et al. Improvement and decline in vision with gene therapy in childhood blindness. *N Engl J Med*. 2015;372(20):1920-1926. doi:10.1056/NEJMoa1412965.
91. Cideciyan A V, Hauswirth WW, Aleman TS, et al. Human RPE65 gene therapy for Leber congenital amaurosis: persistence of early visual improvements and safety at 1 year. *Hum Gene Ther*. 2009;20(9):999-1004. doi:10.1089/hum.2009.086.
92. Hauswirth WW, Aleman TS, Kaushal S, et al. Treatment of leber congenital amaurosis due to RPE65 mutations by ocular subretinal injection of adeno-associated virus gene vector: short-term results of a phase I trial. *Hum Gene Ther*. 2008;19(10):979-990. doi:10.1089/hum.2008.107.
93. Cideciyan A V, Aleman TS, Boye SL, et al. Human gene therapy for RPE65 isomerase deficiency activates the retinoid cycle of vision but with slow rod kinetics. *Proc Natl Acad Sci U S A*. 2008;105(39):15112-15117. doi:10.1073/pnas.0807027105.
94. Hwu W-L, Muramatsu S, Tseng S-H, et al. Gene therapy for aromatic L-amino acid decarboxylase deficiency. *Sci Transl Med*. 2012;4(134):134ra61. doi:10.1126/scitranslmed.3003640.
95. Muramatsu S, Fujimoto K, Kato S, et al. A phase I study of aromatic L-amino acid decarboxylase gene therapy for Parkinson's disease. *Mol Ther*. 2010;18(9):1731-1735. doi:10.1038/mt.2010.135.

96. Wang Z, Zhu T, Qiao C, et al. Adeno-associated virus serotype 8 efficiently delivers genes to muscle and heart. *Nat Biotechnol.* 2005;23(3):321-328. doi:10.1038/nbt1073.
97. Xiao W, Chirmule N, Berta SC, Cullough BMC, Gao G, Wilson JM. Gene Therapy Vectors Based on Adeno-Associated Virus Type 1. *J Virol.* 1999;73(5):3994-4003. <http://jvi.asm.org.ezp.welch.jhmi.edu/content/73/5/3994.full.pdf+html>.
98. Chao H, Liu Y, Rabinowitz J, Li C, Samulski RJ, Walsh CE. Several log increase in therapeutic transgene delivery by distinct adeno-associated viral serotype vectors. *Mol Ther.* 2000;2(6):619-623. doi:10.1006/mthe.2000.0219.
99. Rabinowitz JE, Rolling F, Li C, et al. Cross-packaging of a single adeno-associated virus (AAV) type 2 vector genome into multiple AAV serotypes enables transduction with broad specificity. *J Virol.* 2002;76(2):791-801. doi:10.1128/JVI.76.2.791-801.2002.
100. Nathwani AC, Tuddenham EGD, Rangarajan S, et al. Adenovirus-associated virus vector-mediated gene transfer in hemophilia B. *N Engl J Med.* 2011;365(25):2357-2365. doi:10.1056/NEJMoa1108046.
101. Burnett JR, Hooper AJ. Alipogene tiparvovec, an adeno-associated virus encoding the Ser(447)X variant of the human lipoprotein lipase gene for the treatment of patients with lipoprotein lipase deficiency. *Curr Opin Mol Ther.* 2009;11:681-691.
102. Bryant LM, Christopher DM, Giles AR, et al. Lessons learned from the clinical development and market authorization of Glybera. *Hum Gene Ther Clin Dev.* 2013;24(2):55-64. doi:10.1089/humc.2013.087.
103. Moskalenko M, Chen L, van Roey M, et al. Epitope Mapping of Human Anti-Adeno-Associated Virus Type 2 Neutralizing Antibodies: Implications for Gene Therapy and Virus Structure. *J Virol.* 2000;74(4):1761-1766. doi:10.1128/JVI.74.4.1761-1766.2000.

104. Manning WC, Zhou S, Bland MP, Escobedo JA, Dwarki V. Transient immunosuppression allows transgene expression following readministration of adeno-associated viral vectors. *Hum Gene Ther.* 1998;9(4):477-485. doi:10.1089/hum.1998.9.4-477.
105. Calcedo R, Vandenberghe LH, Gao G, Lin J, Wilson JM. Worldwide epidemiology of neutralizing antibodies to adeno-associated viruses. *J Infect Dis.* 2009;199(3):381-390. doi:10.1086/595830.
106. Benveniste O, Boutin S, Monteilhet V, et al. Prevalence of Serum IgG and Neutralizing Factors Against Adeno-Associated Virus (AAV) Types 1,2,5,6,8, and 9 in the Healthy Population: Implications for Gene Therapy Using AAV Vectors. *Hum Gene Ther.* 2010;21(6):704-712. doi:10.1089/hurn.2009.182.
107. Wang L, Calcedo R, Bell P, et al. Impact of Pre-Existing Immunity on Gene Transfer to Nonhuman Primate Liver with Adeno-Associated Virus 8 Vectors. *Hum Gene Ther.* 2011;22(11):1389-1401. doi:10.1089/hum.2011.031.
108. Calcedo R, Morizono H, Wang L, et al. Adeno-associated virus antibody profiles in newborns, children, and adolescents. *Clin Vaccine Immunol.* 2011;18(9):1586-1588. doi:10.1128/CVI.05107-11.
109. Li C, Narkbunnam N, Samulski RJ, et al. Neutralizing antibodies against adeno-associated virus examined prospectively in pediatric patients with hemophilia. *Gene Ther.* 2012;19(3):288-294. doi:10.1038/gt.2011.90.
110. Murphy SL, Li H, Mingozzi F, et al. Diverse IgG subclass responses to adeno-associated virus infection and vector administration. *J Med Virol.* 2009;81(1):65-74. doi:10.1002/jmv.21360.

111. Labow MA, Hermonat PL, Berns KI. Positive and negative autoregulation of the adeno-associated virus type 2 genome. *J Virol.* 1986;60(1):251-258.  
<http://www.pubmedcentral.nih.gov/articlerender.fcgi?artid=253923&tool=pmcentrez&rendertype=abstract>.
112. Gao G-P, Alvira MR, Wang L, Calcedo R, Johnston J, Wilson JM. Novel adeno-associated viruses from rhesus monkeys as vectors for human gene therapy. *Proc Natl Acad Sci U S A.* 2002;99(18):11854-11859. doi:10.1073/pnas.182412299.
113. Bartel M, Schaffer D, B?ning H. Enhancing the clinical potential of aav vectors by capsid engineering to evade pre-existing immunity. *Front Microbiol.* 2011;2(OCT). doi:10.3389/fmicb.2011.00204.
114. Monteilhet V, Saheb S, Boutin S, et al. A 10 Patient Case Report on the Impact of Plasmapheresis Upon Neutralizing Factors Against Adeno-associated Virus (AAV) Types 1, 2, 6, and 8. *Mol Ther.* 2011;19(11):2084-2091. doi:10.1038/mt.2011.108.
115. Karman J, Gumlaw NK, Zhang J, Jiang JL, Cheng SH, Zhu Y. Proteasome inhibition is partially effective in attenuating pre-existing immunity against recombinant adeno-associated viral vectors. *PLoS One.* 2012;7(4). doi:10.1371/journal.pone.0034684.
116. Mingozzi F, Chen Y, Edmonson SC, et al. Prevalence and pharmacological modulation of humoral immunity to AAV vectors in gene transfer to synovial tissue. *Gene Ther.* 2013;20(4):417-424. doi:10.1038/gt.2012.55.
117. Mimuro J, Mizukami H, Hishikawa S, et al. Minimizing the inhibitory effect of neutralizing antibody for efficient gene expression in the liver with adeno-associated virus 8 vectors. *Mol Ther.* 2013;21(2):318-323. doi:10.1038/mt.2012.258.

118. Mingozi F, Anguela XM, Pavani G, et al. Overcoming preexisting humoral immunity to AAV using capsid decoys. *Sci Transl Med*. 2013;5(194):194ra92. doi:10.1126/scitranslmed.3005795.
119. Anker R, Zavala F, Pollok BA. VH and VL region structure of antibodies that recognize the (NANP)<sub>3</sub> dodecapeptide sequence in the circumsporozoite protein of *Plasmodium falciparum*. *Eur J Immunol*. 1990;20(12):2757-2761. doi:10.1002/eji.1830201233.
120. Balazs AB, Chen J, Hong CM, Rao DS, Yang L, Baltimore D. Antibody-based protection against HIV infection by vectored immunoprophylaxis. *Nature*. 2011;481(7379):81-84. doi:10.1038/nature10660.
121. Balazs AB, Bloom JD, Hong CM, Rao DS, Baltimore D. Broad protection against influenza infection by vectored immunoprophylaxis in mice. *Nat Biotechnol*. 2013;31(7):647-652. doi:10.1038/nbt.2618.
122. Espinosa DA, Gutierrez GM, Rojas-López M, et al. Proteolytic Cleavage of the *Plasmodium falciparum* Circumsporozoite Protein Is a Target of Protective Antibodies. *J Infect Dis*. 2015;212(7):1111-1119. doi:10.1093/infdis/jiv154.
123. Carson S, Miller HB, Witherow DS, Carson S, Miller HB, Witherow DS. Lab Session 5 – DNA Ligation and Transformation of *Escherichia coli*. In: *Molecular Biology Techniques*. ; 2012:35-40. doi:10.1016/B978-0-12-385544-2.00005-3.
124. Palma C, Overstreet MG, Guedon JM, et al. Adenovirus particles that display the *Plasmodium falciparum* circumsporozoite protein NANP repeat induce sporozoite-neutralizing antibodies in mice. *Vaccine*. 2011;29(8):1683-1689. doi:10.1016/j.vaccine.2010.12.040.

125. Scheller LF, Wirtz RA, Azad AF. Susceptibility of different strains of mice to hepatic infection with *Plasmodium berghei*. *Infect Immun*. 1994;62(11):4844-4847.
126. Persson C, Oliveira G a, Sultan A a, Bhanot P, Nussenzweig V, Nardin E. Cutting edge: a new tool to evaluate human pre-erythrocytic malaria vaccines: rodent parasites bearing a hybrid *Plasmodium falciparum* circumsporozoite protein. *J Immunol*. 2002;169(12):6681-6685. doi:10.4049/jimmunol.169.12.6681.
127. Chomczynski P, Sacchi N. Single-step method of RNA isolation by acid guanidinium thiocyanate-phenol-chloroform extraction. *Anal Biochem*. 1987;162(1):156-159. doi:10.1016/0003-2697(87)90021-2.
128. Chomczynski P, Sacchi N. The single-step method of RNA isolation by acid guanidinium thiocyanate – phenol – chloroform extraction : twenty-something years on. *Nat Protoc*. 2006;1(2):581-585. doi:10.1038/nprot.2006.83.
129. Brua-Romero O, Hafalla JCR, Gonzalez-Aseguinolaza G, Sano G ichiro, Tsuji M, Zavala F. Detection of malaria liver-stages in mice infected through the bite of a single *Anopheles* mosquito using a highly sensitive real-time PCR. *Int J Parasitol*. 2001;31(13):1499-1502. doi:10.1016/S0020-7519(01)00265-X.
130. Meliani A, Leborgne C, Triffault S, Jeanson-Leh L, Veron P, Mingozi F. Determination of anti-adenovirus vector neutralizing antibody titer with an in vitro reporter system. *Hum Gene Ther Methods*. 2015;53(April):45-53. doi:10.1089/hgtb.2015.037.
131. Mohammadi ES, Ketner EA, Johns DC, Ketner G. Expression of the adenovirus E4 34k oncoprotein inhibits repair of double strand breaks in the cellular genome of a 293-based inducible cell line. *Nucleic Acids Res*. 2004;32(8):2652-2659. doi:10.1093/nar/gkh593.

132. Kober L, Zehe C, Bode J. Optimized signal peptides for the development of high expressing CHO cell lines. *Biotechnol Bioeng*. 2013;110(4):1164-1173. doi:10.1002/bit.24776.
133. Burton DR, Gregory L, Jefferis R. Aspects of the molecular structure of IgG subclasses. *Monogr Allergy*. 1986;19:7-35. <http://www.ncbi.nlm.nih.gov/pubmed/2945094>. Accessed March 14, 2016.
134. Salvador A, Hernández RM, Pedraz JL, Igartua M. Plasmodium falciparum malaria vaccines: current status, pitfalls and future directions. *Expert Rev Vaccines*. 2012;11(9):1071-1086. doi:10.1586/erv.12.87.
135. Gao G, Alvira MR, Somanathan S, et al. Adeno-associated viruses undergo substantial evolution in primates during natural infections. *Proc Natl Acad Sci U S A*. 2003;100(10):6081-6086. doi:10.1073/pnas.0937739100.
136. Nieto K, Stahl-Hennig C, Leuchs B, Müller M, Gissmann L, Kleinschmidt J a. Intranasal Vaccination with AAV5 and 9 Vectors Against Human Papillomavirus Type 16 in Rhesus Macaques. *Hum Gene Ther*. 2012;23(July):733-741. doi:10.1089/hum.2011.202.
137. Sondhi D, Johnson L, Purpura K, et al. Long-Term Expression and Safety of Administration of AAVrh.10hCLN2 to the Brain of Rats and Nonhuman Primates for the Treatment of Late Infantile Neuronal Ceroid Lipofuscinosis. *Hum Gene Ther Methods*. 2012;23(5):324-335. doi:10.1089/hgtb.2012.120.
138. Calcedo R, Wilson JM. Humoral Immune Response to AAV. *Front Immunol*. 2013;4. doi:10.3389/fimmu.2013.00341.

139. Zinn E, Pacouret S, Khaychuk V, et al. In silico reconstruction of the viral evolutionary lineage yields a potent gene therapy vector. *Cell Rep.* 2015;12(6):1056-1068. doi:10.1016/j.celrep.2015.07.019.
140. Manno CS, Pierce GF, Arruda VR, et al. Successful transduction of liver in hemophilia by AAV-Factor IX and limitations imposed by the host immune response. *Nat Med.* 2006;12(3):342-347. doi:10.1038/nm1358.
141. Vandenberghe LH, Wang L, Somanathan S, et al. Heparin binding directs activation of T cells against adeno-associated virus serotype 2 capsid. *Nat Med.* 2006;12(8):967-971. doi:10.1038/nm1445.
142. Herzog RW, Fields P a, Arruda VR, et al. Influence of vector dose on factor IX-specific T and B cell responses in muscle-directed gene therapy. *Hum Gene Ther.* 2002;13(11):1281-1291. doi:10.1089/104303402760128513.
143. Maguire AM, Simonelli F, Pierce EA, et al. Safety and efficacy of gene transfer for Leber's congenital amaurosis. *N Engl J Med.* 2008;358(21):2240-2248. doi:10.1056/NEJMoa0802315.



## Curriculum Vitae

RENUKA ELIZABETH JOSEPH

Date of birth – June 9<sup>th</sup> 1991

Place of birth –Ernakulam, Kerala, India

101 West Read Street, Apt. 611 | Baltimore, MD 21201

renukajoseph91@gmail.com

### **EDUCATION**

JOHNS HOPKINS BLOOMBERG SCHOOL OF PUBLIC HEALTH

**ScM in Molecular Microbiology and Immunology** | 2014-2016

- Completed six months rotation in the Sinnis lab where the main focus is on the skin stage of malarial parasites. My rotation project's main goal was to study the effects of an antibody 2F6 on *Plasmodium yoelii* liver load in vivo. 2F6 is thought to bind at the repeat region of the Circumsporozoite protein of *P.yoelii* and inhibit the sporozoites from entering the blood vessels and in turn the liver.
- Studied the process to purify antibody from ascites and did some initial experiments to study the half-life of 2F6. Worked on mosquitoes and mice during lab rotations.
- Decided to carry out thesis project in the Ketner lab that is currently working on a vectored immunoprophylaxis against *Plasmodium falciparum* infection. The vector, in this case, is adeno-associated virus and it delivers anti-*P. falciparum* monoclonal antibody genes, which act on the Circumsporozoite protein of the sporozoite preventing further progression of the malarial parasite life cycle in the host. Through this project, I studied the design and preparation of plasmids, worked with tissue culture and also with

viruses.

- Currently working on a luciferase assay to detect the presence of neutralizing antibodies against the vector before immunization with this treatment as a side project. The presence of the neutralizing antibodies may play a role in the effectiveness of this treatment and it could also help in deciding which vector should be used for immunization.
- Performed and asserted responsibilities of a teaching assistant in the course introduction to biomedical sciences both for the online and onsite version. Graded and discussed class materials in the context of real-world problems (online version) and conducted 2 lectures on Hematology and the reproductive system (on-site version).
- Acquired a certificate in good clinical practices and in vaccine development and policy from Johns Hopkins Bloomberg School of Public Health.

## VELLORE INSTITUTE OF TECHNOLOGY

### **Bachelor of Technology - Specializing in Biotechnology | 2009-2013**

Graduating CGPA – 3.43; Excelled in my final thesis project securing one of the highest marks in my class - 97%

### **PUBLICATIONS/ PRESENTATIONS/CONFERENCES**

- Participated and presented a research paper in the 3rd International Conference on Science, Engineering and Technology (SET) entitled "A preliminary study and first report on caffeine-degrading bacteria isolated from the soils of Chittoor and Vellore," which was published in the *International Research Journal of Pharmacy* in 2012.
- Thesis was made into a paper entitled "Screening and molecular characterization of *Serratia marcescens* VITSD2: A strain producing optimum serratiopeptidase" and was

published in the journal *Frontiers in Biology* in 2014.

- A review paper entitled “Leishmaniasis: A Review on Global Epidemiological trends” was published in the *Research Journal of Pharmacy and Technology* in 2014.
- Worked on a project that studied the possible relationship between environment, gender and Internet addiction.
- Worked on the construction of a microbial fuel cell from a consortium of bacteria as a part of the team that participated in the International Genetically Engineered Machine Competition in 2012 from VIT University.
- Did a summer project on the cloning of *arsR* gene into *Escherichia coli* (DH5alpha) to create a pH sensitive color-based arsenic biosensor to test the contamination of water by arsenic.
- Participated in the VIT Bio Summit in 2012.
- One of the comperes for the Science Academics Lecture Workshop on "Mineral Microbes and Environment.”

### **INTERNSHIP EXPERIENCE**

**Kemin Industries South Asia Private Limited** (*summer internship*) | Chennai, India.

- Worked on projects that dealt with probiotics and on the development of a vaccine for infectious diseases found in poultry.

**Thrombosis Research Institute** | Bengaluru, Karnataka, India

- Contributed in this charitable institution conducting studies to combat the life-threatening effects of thrombosis.

## **LANGUAGES**

- English
- Hindi
- Malayalam
- French